SNLS3: Constraints on Dark Energy Combining the Supernova Legacy Survey Three Year Data with Other Probes

M. Sullivan[1], J. Guy[2], A. Conley[3,4], N. Regnault[2], P. Astier[2], C. Balland[2,5], S. Basa[6],
R. G. Carlberg[3], D. Fouchez[7], D. Hardin[2], I. M. Hook[1,8], D. A. Howell[9,10], R. Pain[2],
N. Palanque-Delabrouille[11], K. M. Perrett[3,12], C. J. Pritchet[13], J. Rich[11], V. Ruhlmann-Kleider[11],
D. Balam[13], S. Baumont[14], R. S. Ellis[15,1], S. Fabbro[13], H. K. Fakhouri[17], N. Fourmanoit[2],
S. González-Gaitán[3], M. L. Graham[9,10], M. J. Hudson[18,19], E. Hsiao[17], T. Kronborg[2],
C. Lidman[20], A. M. Mourao[16], J. D. Neill[21], S. Perlmutter[17,22], P. Ripoche[17,2], N. Suzuki[17],
E. S. Walker[1,22]

sullivan@astro.ox.ac.uk

ABSTRACT

We present observational constraints on the nature of dark energy using the Supernova Legacy Survey three year sample (SNLS3) of Guy et al. (2010) and Conley et al.

---

[1]Department of Physics (Astrophysics), University of Oxford, Keble Road, Oxford, OX1 3RH, UK

[2]LPNHE, Université Pierre et Marie Curie Paris 6, Université Paris Diderot Paris 7, CNRS-IN2P3, 4 place Jussieu, 75252 Paris Cedex 05, France

[3]Department of Astronomy and Astrophysics, University of Toronto, 50 St. George Street, Toronto, ON M5S 3H4, Canada

[4]Center for Astrophysics and Space Astronomy, University of Colorado, 593 UCB, Boulder, CO 80309-0593, USA

[5]Université Paris 11, Orsay, F-91405, France

[6]LAM, CNRS, BP8, Pôle de l'Étoile Site de Château-Gombert, 38, rue Frédéric Joliot-Curie, 13388 Marseille Cedex 13, France

[7]CPPM, Aix-Marseille Université, CNRS/IN2P3, Marseille, France

[8]INAF - Osservatorio Astronomico di Roma, via Frascati 33, 00040 Monteporzio (RM), Italy

[9]Las Cumbres Observatory Global Telescope Network, 6740 Cortona Dr., Suite 102, Goleta, CA 93117, USA

[10]Department of Physics, University of California, Santa Barbra, Broida Hall, Mail Code 9530, Santa Barbara, CA 93106-9530, USA

[11]CEA, Centre de Saclay, Irfu/SPP, F-91191 Gif-sur-Yvette, France

[12]Network Information Operations, DRDC Ottawa, 3701 Carling Avenue, Ottawa, ON, K1A 0Z4, Canada

[13]Department of Physics and Astronomy, University of Victoria, PO Box 3055 STN CSC, Victoria BC, V8T 1M8, Canada

[14]LPSC, UJF, CNRS/IN2P3, INPG, 53 rue des Martyrs, 38026 Grenoble Cedex, France

[15]Department of Astrophysics, California Institute of Technology, MS 105-24, Pasadena, CA 91125, USA

[16]CENTRA-Centro Multidisciplinar de Astrofísica and Dep. Física, IST, Av. Rovisco Pais, 1049-001 Lisboa, Portugal

[17]LBNL, 1 Cyclotron Rd, Berkeley, CA 94720

[18]Department of Physics and Astronomy, University of Waterloo, 200 University Avenue West, Waterloo, Ontario N2L 3G1, Canada

[19]Perimeter Institute for Theoretical Physics, 31 Caroline St. N., Waterloo, ON, N2L 2Y5, Canada

[20]Australian Astronomical Observatory, P.O. Box 296, Epping, NSW 1710, Australia

[21]California Institute of Technology, 1200 E. California Blvd., Pasadena, CA 91125, USA

[22]Department of Physics, University of California, Berkeley, 366 LeConte Hall MC 7300, Berkeley, CA 94720-7300, USA

[23]Scuola Normale Superiore, Piazza dei Cavalieri 7, 56126 Pisa, Italy

(2011). We use the 472 SNe Ia in this sample, accounting for recently discovered correlations between SN Ia luminosity and host galaxy properties, and include the effects of all identified systematic uncertainties directly in the cosmological fits. Combining the SNLS3 data with the full WMAP7 power spectrum, the Sloan Digital Sky Survey luminous red galaxy power spectrum, and a prior on the Hubble constant H_0 from SHOES, in a flat universe we find $\Omega_m = 0.269 \pm 0.015$ and $w = -1.061^{+0.069}_{-0.068}$ – a 6.5% measure of the dark energy equation-of-state parameter w. The statistical and systematic uncertainties are approximately equal, with the systematic uncertainties dominated by the photometric calibration of the SN Ia fluxes – without these calibration effects, systematics contribute only a $\sim 2\%$ error in w. When relaxing the assumption of flatness, we find $\Omega_m = 0.271 \pm 0.015$, $\Omega_k = -0.002 \pm 0.006$, and $w = -1.069^{+0.091}_{-0.092}$. Parameterizing the time evolution of w as $w(a) = w_0 + w_a(1 - a)$, gives $w_0 = -0.905 \pm 0.196$, $w_a = -0.984^{+1.094}_{-1.097}$ in a flat universe. All of our results are consistent with a flat, $w = -1$ universe.

The size of the SNLS3 sample allows various tests to be performed with the SNe segregated according to their light curve and host galaxy properties. We find that the cosmological constraints derived from these different sub-samples are consistent. There is evidence that the coefficient, β, relating SN Ia luminosity and color, varies with host parameters at $> 4\sigma$ significance (in addition to the known SN luminosity–host relation); however this has only a small effect on the cosmological results and is currently a subdominant systematic.

Subject headings: cosmology: observations – cosmological parameters – supernovae: general – surveys

1. Introduction

The discovery of the accelerating universe ranks as one of science's landmark achievements in the 20th century. Surveys exploiting distant Type Ia supernovae (SNe Ia) as standardizable candles (Riess et al. 1998; Perlmutter et al. 1999) revealed the presence of a "dark energy" that opposes gravity and accelerates the expansion of the Universe. When these SN observations are combined with measures of large-scale structure (Cole et al. 2005; Eisenstein et al. 2005; Percival et al. 2007; Reid et al. 2010) and the cosmic microwave background (CMB; e.g., de Bernardis et al. 2002; Bennett et al. 2003; Larson et al. 2011), this dark energy emerges as the dominant component of the Universe responsible for 70–75% of its energy density at the present epoch.

A compelling physical explanation of dark energy remains distant despite a range of possibilities being postulated (for reviews see Copeland et al. 2006; Frieman et al. 2008). Astrophysical measurements of the dark energy's equation-of-state parameter w (the ratio of its pressure to density, p/ρ), and its variation over cosmic history, can help distinguish the possibilities. The classical

"Cosmological Constant" is equivalent to a vacuum energy density with negative pressure, constant in time and space: $w = -1$. The broad family of "quintessence" models, a dynamical form of scalar energy field, mostly predict $-1 \leq w < -\frac{1}{3}$. A measurement of $w < -1$ would be a signal of even more exotic physics.

SNe Ia remain, at present, the most direct and mature method of probing this dark energy due to several decades of intensive study and use in cosmology (see the review of Howell 2010). Thought to be the result of the thermonuclear destruction of an accreting CO white dwarf star approaching the Chandrasekhar mass limit (e.g., Hillebrandt & Niemeyer 2000), they are standardizable candles which explode with nearly the same brightness everywhere in the Universe due to the uniformity of the triggering mass and hence the available nuclear fuel. Their cosmological use exploits simple empirical relations between their luminosity and other parameters. Brighter SNe Ia have slower, wider light curves (Phillips 1993) and are typically bluer than their faster, fainter counterparts (Riess et al. 1996; Tripp 1998). Detailed searches for a "third parameter" have recently shown that, after applying these first two corrections, brighter SNe Ia reside in more massive host galaxies (Kelly et al. 2010; Sullivan et al. 2010; Lampeitl et al. 2010).

The application of relations between SN Ia light-curve-shape, color, and host galaxy properties provides robust distance estimates which allow SNe Ia to be used to measure cosmological parameters. When combined together, recent SN Ia samples (Astier et al. 2006; Riess et al. 2007; Miknaitis et al. 2007; Holtzman et al. 2008; Hicken et al. 2009a; Contreras et al. 2010) provide measures of dark energy generally consistent with a cosmological constant of $w = -1$ with statistical uncertainties in w of around 5–7%, and systematic uncertainties of 8–14%, depending on the method used and assumptions made (Kessler et al. 2009; Hicken et al. 2009b; Amanullah et al. 2010). These SN Ia samples are now sufficiently large that our understanding of systematic uncertainties has a direct impact on our measurement of dark energy (Kessler et al. 2009; Conley et al. 2011), particularly when combining SNe Ia from many different surveys at different observatories.

Systematic uncertainties which affect the cosmological analysis of SNe Ia arise from two broad sources. The first is experimental systematics; for example, photometric calibration or survey selection biases. Due to the correlations between SN Ia magnitudes that these uncertainties introduce, accounting for their effects in the cosmological fits is particularly important. Fortunately this is a tractable problem as the uncertainties are understood in modern SN Ia samples and can be accurately modeled, albeit only after detailed and painstaking work (Regnault et al. 2009; Guy et al. 2010; Conley et al. 2011). The second source of systematics arises from an incomplete understanding of their astrophysics (e.g., progenitor configuration, mass transfer and explosion mechanism, etc.). The most pernicious possibilities include evolution in SN Ia properties with redshift tracking changing metallicities/ages of the progenitor stars, and varying dust extinction or color laws; the correct treatment of SN Ia color–luminosity relationships are particularly uncertain (e.g., Conley et al. 2007). The effects of these potential systematics are more nebulous due to the difficulty in modeling SNe Ia explosions, but can be investigated empirically. Studies which compare local SN Ia spectra with those at high-redshift find a remarkable degree of similarity across 2780Å to 6000Å

(Hook et al. 2005; Blondin et al. 2006; Foley et al. 2008; Ellis et al. 2008; Balland et al. 2009; Cooke et al. 2011) with only small differences in the strengths of some intermediate mass element features (Sullivan et al. 2009), consistent with a mildly evolving mix in SN Ia demographics with redshift expected from popular SN Ia delay-time distribution models (Mannucci et al. 2005; Sullivan et al. 2006b; Mannucci et al. 2006; Howell et al. 2007). To date, no definitive evolutionary signature with redshift, which would directly impact a cosmological analysis, has been located.

This paper presents the cosmological analysis of the three year Supernova Legacy Survey SN Ia sample (SNLS3). Our sample and methods are presented over the course of several papers. The first, Regnault et al. (2009), deals with the photometric calibration of the SNLS SN Ia fluxes and associated systematic uncertainties, including corrections for spatial non-uniformities in the SNLS photometric imager. Guy et al. (2010, hereafter G10), presents the light curves of the SNLS SNe Ia themselves, together with a comparison of SN light curve fitting techniques, color laws, systematics and parameterizations. Conley et al. (2011, hereafter C11), discusses systematic effects in the cosmological analysis (including covariance matrices accounting for correlations between the distances to different SNe), presents light curve parameterizations of external SNe Ia used in the analysis, describes the various light curve quality cuts made to produce the combined sample, and provides the cosmological constraints obtained from the SN Ia data alone. Other papers describe the SNLS selection biases (Perrett et al. 2010), the SN Ia host galaxy information (Sullivan et al. 2010), and the spectroscopic confirmation and redshift measurements (Howell et al. 2005; Bronder et al. 2008; Balland et al. 2009; Walker et al. 2011). This paper performs a cosmological analysis combining the SN-only analysis of C11 with other external, non-SNe constraints.

We use 242 well-sampled SNe Ia over $0.08 < z < 1.06$ from the SNLS together with a large literature sample: 123 SNe Ia at low-redshift, 14 SNe Ia at $z \gtrsim 0.8$ from the Hubble Space Telescope, and 93 SNe Ia at intermediate redshift from the first year of the Sloan Digital Sky Survey-II SN search. We include the effects of identified systematic uncertainties directly in our cosmological fitting analysis using an approach outlined in detail in C11. This allows our cosmological parameter uncertainties to include systematic as well as statistical uncertainties, with covariances between different SNe which influence the cosmological fits accounted for. Examples of effects which cause such covariances include common photometric zeropoints for different SNe, or selection effects for SNe from the same survey. Appropriate covariance matrices allowing other users of this combined data set to directly include systematic effects in subsequent analyses can be found in C11.

The advantages of the enlarged SNLS data set are multiple. Most obviously, this represents a threefold increase in the SNLS sample size compared to the first year SNLS cosmological analysis presented in Astier et al. (2006, hereafter A06), and as such provides a significant improvement in the statistical precision of the cosmological constraints. Several improvements in survey strategy were made following the first year of SNLS, including a more regular observing cadence together with longer z-band exposures, important for the highest redshift events. Moreover, the enlarged data set allows sources of potential astrophysical systematics to be examined by dividing our SN Ia sample according to properties of either the SN (e.g., light curve width) or its environment (Sullivan

et al. 2010). The increased size of the SNLS data set has also enabled a better understanding of SN Ia light curve and spectral properties (particularly at $\lambda < 3600$Å in the rest-frame) with a corresponding improvement in the methods for estimating their distances (Hsiao et al. 2007; Guy et al. 2007; Ellis et al. 2008; Conley et al. 2008), and handling their colors (G10). The full three years of the SNLS data also allow an improved photometric calibration of the light curves and a more consistent understanding of the experimental characteristics (Regnault et al. 2009).

A plan of the paper follows. § 2 provides a brief overview of the SN Ia data, and § 3 describes our methodology for determining the cosmological parameters. Our cosmological results are presented in § 4. § 5 discusses cosmological fits to various sub-samples of our SN population designed to assess possibilities of astrophysical biases within the SN Ia sample. We summarize and conclude in § 6.

2. Supernova Data and Methodology Overview

We begin by briefly reviewing the SN Ia datasets and the various techniques that we use in the cosmological analysis. Full details of all of our procedures can be found in G10 and C11, as well as Guy et al. (2007), Conley et al. (2008), Perrett et al. (2010), and Sullivan et al. (2010).

2.1. The SN Ia samples

Our SN Ia samples are divided into two categories: those discovered and confirmed by the Supernova Legacy Survey (SNLS), and those taken from the literature which sample different redshift ranges to SNLS. The SNLS uses data taken as part of the five-year Canada-France-Hawaii Telescope Legacy Survey (CFHT-LS). CFHT-LS is an optical imaging survey, the deep component of which conducted repeat imaging of 4 fields every 3–4 nights in dark time with four filters, allowing the construction of high-quality multi-color SN light curves (G10). Spectroscopic follow-up is used to confirm SN types and measure redshifts, critical in obtaining clean samples of SNe Ia as reliable photometric identification techniques have yet to be developed, despite recent progress (Kessler et al. 2010; Bazin et al. 2011). Candidates were prioritized following the procedure outlined in Sullivan et al. (2006a). SNLS benefited from large time allocations on 8–10m class telescopes – ~ 1500 hours over five years – including the Gemini North and South telescopes, the European Southern Observatory Very Large Telescopes, and the Keck telescopes. Nearly all our SN spectra are published[1] (Howell et al. 2005; Bronder et al. 2008; Ellis et al. 2008; Balland et al. 2009; Walker et al. 2011). All spectra are analyzed and uniformly typed according to the classification schemes of Howell et al. (2005) and Balland et al. (2009). Further information on all 242 SNLS SNe Ia that

---

[1] Spectra and light curves for the SNLS3 sample are available at the University of Toronto's Research Repository, T-Space: https://tspace.library.utoronto.ca/snls, as well as in the cited papers.

we use, including light curve parameterizations, can be found in G10.

The SNLS dataset is complemented with SNe Ia from the literature over redshift ranges that the SNLS sample does not cover. We use 123 SNe Ia at low-redshift ($z \lesssim 0.08$) from a variety of sources (primarily Hamuy et al. 1996; Riess et al. 1999; Jha et al. 2006; Hicken et al. 2009a; Contreras et al. 2010), 14 SNe Ia at $z \gtrsim 0.8$ from the HST-discovered sample of Riess et al. (2007), and 93 SNe Ia over $0.06 \lesssim z \lesssim 0.4$ from the first year of the Sloan Digital Sky Survey-II SN search (Holtzman et al. 2008). Light curve parameterizations and other data for these events, on the same relative system as that of G10, can be found in C11.

We also considered including other SN Ia samples that, at least in part, probe the same redshift range as SNLS. However, we do not do this for several reasons (see also C11 for a discussion of these points). SNLS is designed to control systematics as much as is possible – a single telescope survey with a well-understood photometric response and calibration, using deep exposures in filters that allow the same rest-frame colors to be measured for most of the redshift range that it probes. There is also significant published information on the host galaxies (Sullivan et al. 2010), essential for the cosmological analysis and which is not available for other higher-redshift samples. Finally, SNLS is by far the largest and best observed (i.e., highest signal-to-noise for each event) SN Ia sample over $0.3 \lesssim z \lesssim 1.0$. Adding other SNe to this might lead to marginally improved cosmological constraints from a purely statistical perspective, but would certainly lead to a much more complex and uncertain analysis of systematic uncertainties when combining data from many surveys conducted at many telescopes.

All SNe are corrected for Galactic extinction, Malmquist and other selection biases (Perrett et al. 2010; Conley et al. 2011), and peculiar velocities (at low redshift).

2.2. Light curve fitting

We parameterize the SN Ia light curves for distance estimation using the combined results from updated versions of two independent light curve fitters – SiFTO (Conley et al. 2008) and SALT2 (Guy et al. 2007). Both techniques provide an estimate of the SN peak rest-frame B-band apparent magnitude at the epoch of maximum light in that filter, a measure of the SN light curve shape, and an estimate of the SN optical $B - V$ color ($\mathcal{C}$). SiFTO parameterizes the light curve in terms of stretch (s), while SALT2 uses a related parameter x_1. The two light curve fitters are compared in G10, which also provides details of the techniques we used to average them into a single light curve parameterization.

We apply various selection cuts to the SN Ia samples designed to ensure an adequate wavelength and phase coverage in the light curve fits. These are described in detail in G10 and C11, and essentially ensure that an accurate light curve width, rest-frame color, and peak rest-frame B-magnitude can be measured. Additionally, each SN must be spectroscopically confirmed (see Howell et al. 2005, for a discussion of our spectroscopic classification criteria), have a minimum CMB-

frame redshift (z_{cmb}) of 0.010 (after peculiar velocity correction), be spectroscopically normal, have a Galactic extinction of $E_{B-V}^{\mathrm{mw}} < 0.2$, and be of normal stretch ($0.7 < s < 1.3$) and color ($-0.25 < \mathcal{C} < 0.25$). We also remove 6 outliers on the Hubble diagram – see C11 for details.

2.3. Host galaxy parameterizations

Recent analyses have found correlations between SN Ia luminosity and their host galaxies, even after the well-known fainter–faster and fainter–redder corrections have been made (Kelly et al. 2010; Sullivan et al. 2010; Lampeitl et al. 2010). At the present time, it is not clear from an astrophysical perspective which host galaxy parameter is the optimal choice to use (as the third parameter) in the analysis. The observed effects could be due to progenitor metallicity (e.g., Kasen et al. 2009), progenitor age (e.g., Krueger et al. 2010), or possibly some other parameter. Empirically, trends in SN Ia luminosity are seen with a variety of derived host galaxy parameters, including stellar mass (M_{stellar}), star formation rate (SFR), and inferred stellar age. However many of these parameters are strongly correlated when derived from broad-band photometry available for the host galaxies.

We use the host galaxy stellar mass as the third variable in our cosmological fitting. This has the advantage of being easiest to determine from sometimes limited host data, and shows significant trends with the SN Ia luminosities. We derive the host information by following the method in Sullivan et al. (2010), fitting the broad-band spectral energy distribution (SED) of the host galaxies using simple galaxy population synthesis models (Le Borgne & Rocca-Volmerange 2002). The host galaxy information can be found in G10 and C11 for all the SNe used in our analysis.

2.4. Systematic uncertainties

We consider a variety of systematic uncertainties in our analysis, discussed in detail in C11. Details of the construction of the covariance matrices that encode this information can be found in that paper. For each systematic we estimate its size and adjust that variable in the light curve fits. All the light curves are refit, including a re-training of the light curve model where required, and the derived light curve parameters (m_B, s, $\mathcal{C}$) compared for each SN with and without the inclusion of the systematic. These differences are converted into a covariance matrix following C11.

3. Cosmological fit methodology

Having summarized the main features of our dataset, we now turn to the cosmological analysis. The cosmological fit minimizes

$$\chi^2 = \sum_{\mathrm{SNe}} \frac{\left(m_B - m_B^{\mathrm{mod}}\right)^2}{\sigma_{\mathrm{stat}}^2 + \sigma_{\mathrm{int}}^2} \tag{1}$$

where we have omitted the covariance error matrix for clarity. $\sigma_{\rm stat}$ is the identified statistical error and includes uncertainties in both m_B and $m_B^{\rm mod}$, $\sigma_{\rm int}$ parameterizes the intrinsic dispersion of each SN sample (see below), and the sum is over the SNe Ia entering the fit. m_B are the maximum-light SN rest-frame B-band apparent magnitudes and $m_B^{\rm mod}$ are the model B-band magnitudes for each SN given by

$$m_B^{\rm mod} = 5 \log_{10} \mathcal{D}_L \left(z_{\rm hel}, z_{\rm cmb}, w, \Omega_m, \Omega_{\rm DE}, \Omega_k\right) \tag{2}$$
$$-\alpha \left(s - 1\right) + \beta \mathcal{C} + \mathcal{M}_B$$

where w is the equation of state parameter of dark energy, Ω_m and $\Omega_{\rm DE}$ are the fractional energy densities of matter and dark energy (for $w = -1$, $\Omega_{\rm DE} \equiv \Omega_\Lambda$), Ω_k is the curvature constant, and α and β parameterize the s and $\mathcal{C}$–luminosity relationships. Any linear variation between SN intrinsic color and s is allowed for and will be absorbed into the α term. $z_{\rm hel}$ is the heliocentric redshift used in the light curve fits. $\mathcal{D}_L$ is the c/H_0 reduced luminosity distance with the c/H_0 factor absorbed into $\mathcal{M}_B$ (here c is the speed of light and H_0 the Hubble constant). Explicitly, $\mathcal{M}_B = M_B + 5 \log_{10}(c/H_0) + 25$, where M_B is the rest-frame absolute magnitude of a SN Ia in the B-band. Neither H_0 nor M_B are assumed during the fitting process.

We allow $\mathcal{M}_B$ to vary as a function of host galaxy stellar mass ($\rm M_{stellar}$) to account for relations between SN Ia brightness and host properties that are not corrected for via the standard s and $\mathcal{C}$–luminosity relations following Sullivan et al. (2010). Explicitly, we fit for $\mathcal{M}_B^1$ in galaxies with $\rm M_{stellar} \leq 10^{10}\,M_\odot$, and $\mathcal{M}_B^2$ when $\rm M_{stellar} > 10^{10}\,M_\odot$. We could, of course, allow the other nuisance parameters α and β to vary according to host type – we discuss this further in § 5.

The statistical errors affecting each SN include the statistical error in m_B from the light curve fit, the statistical error in $m_B^{\rm mod}$ (essentially $\alpha\sigma_s$ and $\beta\sigma_\mathcal{C}$), a peculiar velocity error of 150 $\rm km\,s^{-1}$ after correction for a local bulk flow model, the error in $z_{\rm hel}$ projected into magnitude space, a 10% uncertainty from Milky Way extinction corrections (Schlegel et al. 1998), a random scatter due to gravitational lensing following Jönsson et al. (2010) of $\sigma_{\rm lens} = 0.055z$, and the covariances between s, $\mathcal{C}$ and m_B for an individual SN (these parameters are correlated as they are determined from the same light curve data). $\sigma_{\rm stat}$ is updated during the fits as α and β are altered. The $\sigma_{\rm int}$ term parameterizes the extra dispersion in m_B required to give a χ^2 per degree of freedom (DOF) of one in the cosmological fits (e.g., Perlmutter et al. 1999). This "intrinsic" dispersion arises from unidentified sources of error in our analysis, as well as the imperfect nature of SNe Ia as standard candles. $\sigma_{\rm int}$ may also include contributions from unidentified experimental errors and there is no *a priori* reason for $\sigma_{\rm int}$ to be the same from SN sample to SN sample; we allow a different $\sigma_{\rm int}$ for each sample, the values for which can be found in table 4 of C11. These values are not varied in the fits, but the values are fixed to give a $\chi^2/{\rm DOF} = 1$ for each sample in the SN only cosmological fits of Conley et al. (2011).

To include systematic errors we generalize eqn. (1) by constructing a covariance matrix $\mathbf{C}$ to replace the σ terms. $\mathbf{C}$ is the combination of a systematics covariance matrix $\mathbf{C}_{\rm syst}$ and two covariance matrices containing statistical uncertainties: $\mathbf{C}_{\rm stat}$ which contains statistical errors from

the SN model used in the light curve fit and which are therefore correlated between SNe, and $\mathbf{D}_{\mathrm{stat}}$, a purely diagonal covariance matrix generated from the statistical errors described above. We include both $\mathbf{C}_{\mathrm{stat}}$ and $\mathbf{D}_{\mathrm{stat}}$ when performing fits based only on statistical errors.

We then minimize the χ^2 according to

$$\chi^2 = \sum_N \left(\vec{\mathbf{m_B}} - \vec{\mathbf{m_B^{\mathrm{mod}}}} \right)^T \mathbf{C}^{-1} \left(\vec{\mathbf{m_B}} - \vec{\mathbf{m_B^{\mathrm{mod}}}} \right) \tag{3}$$

This methodology allows the quoted uncertainties on the fit parameters to directly include systematic errors, as well as correctly accounting for systematic and statistical uncertainties which induce correlations between different SNe and thus alter the position of the best-fit cosmological model.

3.1. Fitting techniques

We use three approaches[2] to perform our cosmological fits. For relatively simple cosmological fits involving a small number of parameters, we use a grid technique that computes the χ^2 of eqn. (3) at every point converting into a probability via $P \propto \exp\left(-\frac{1}{2}\chi^2\right)$, with the proportionality set by normalizing over the grid. The "nuisance parameters" α, β and $\mathcal{M}_B$ are marginalized over when generating confidence contours in the parameters of interest, and we report the expectation value of the marginalized parameters. Due to the (relatively) fast run-time, and the contour visualization, this fitting technique is particularly well-suited to analyzing the magnitude of the individual sources of systematic uncertainty in our analysis, which would be impractical with more complex and slower fitting approaches.

The second approach is a χ^2 minimization routine which simply reports the best-fit. The results of this technique should be close to the reported values from the grid marginalization, but should not be expected to agree exactly, and we provide both. Note that the σ_{int} calculated by C11 is performed for the marginalization approach fits – when these σ_{int} are used in the χ^2 minimization fits, a $\chi^2/\mathrm{DOF} < 1$ should be expected as the best-fit parameters from the marginalization fits will not lie at a minimum in χ^2.

The third approach is the `CosmoMC` program (Lewis & Bridle 2002), which uses a Markov-Chain Monte Carlo technique to explore cosmological parameter space. We use this approach for our main cosmological results. We made the following modifications to the May 2010 version of `CosmoMC` package to handle SNLS3 data: first, we properly marginalize over the SN nuisance parameters α and β rather than holding them fixed; second, we keep track of the difference between heliocentric and CMB frame redshifts, which enter into the luminosity distance differently, important for some

---

[2]All the computer programs and code referred to in this paper are available at https://tspace.library.utoronto.ca/snls, along with the SN Ia light curves, spectra, light-curve parameters, covariance matrices, and some of the `CosmoMC` chains.

of the lowest-z SNe; third, we have added the ability to fit for the host-dependence of SN Ia absolute luminosities as described in Sullivan et al. (2010).

The first item above is handled most efficiently by explicitly fitting for α and β along with the cosmological parameters, as internally marginalizing over their values is computationally more expensive for the SNLS3 sample. The consequences of incorrectly holding the nuisance variables fixed, or of simply substituting the values that minimize the χ^2, both true of the default `CosmoMC` SN Ia implementation, are discussed in section 4.6 and Appendix C of C11, as well as § 4 of this paper. In brief, this simplified approach leads to both underestimated uncertainties, and biased parameter estimates, due to small correlations between α, β, and the cosmological parameters.

For `CosmoMC` fits where we allow for a time-varying dark energy equation of state ($w(a) = w_0 + w_a(1 - a)$, where a is the scale factor), we follow the prescription of Fang et al. (2008). Further, in the `CosmoMC` fits we do not consider massive neutrinos, and assume a simple power-law primordial power spectrum (i.e., we neglect tensor modes, and any running of the scalar spectral index).

3.2. External, non-SN datasets

We include several external non-SN datasets in our fits. For the grid marginalization and χ^2 minimization fits, we use two external constraints. The first is the Sloan Digital Sky Survey (SDSS) Data Release 7 (DR7) Baryon Acoustic Oscillations (BAO) measurements of Percival et al. (2010). This is a Gaussian prior on the distance ratios $r_s(z_d)/D_V(z)$ at $z = 0.2$ and $z = 0.35$, where $r_s(z_d)$ is the comoving sound horizon at the baryon drag epoch, and $D_V(z)$ is a spherically averaged effective distance measure given by $D_V(z) = [(1 + z)^2 D_A^2(z) cz/H(z)]^{1/3}$ (Eisenstein et al. 2005) where $D_A(z)$ is the proper angular diameter distance. The second is a prior based on the Wilkinson Microwave Anisotropy Probe 7-year (WMAP7) "shift" parameter R, the "acoustic scale" l_a, and the decoupling redshift z_*, as defined in Komatsu et al. (2011), following the prescription of Komatsu et al. (2009). This prior includes most of the power of the WMAP7 data for measuring dark energy.

For our main cosmological fits, with the `CosmoMC` program, we use different external constraints: the power spectrum of luminous red galaxies (LRGs) in the SDSS DR7 (Reid et al. 2010) in place of the BAO constraints, the full WMAP7 CMB power spectrum (Larson et al. 2011) in place of the shift parameters, and a prior on H_0 from the SHOES (Supernovae and H_0 for the Equation of State) program (Riess et al. 2009, 2011). This Gaussian H_0 prior, $H_0 = 73.8 \pm 2.4$ km s^{-1} Mpc^{-1}, makes use in its construction of many of the low-redshift $z < 0.1$ SNe Ia used in this paper. Their absolute magnitudes are calibrated directly using Cepheid variables in eight local SN Ia host galaxies (Riess et al. 2011), the Cepheids themselves calibrated using different techniques: the geometric maser distance to the galaxy NGC 4258, trigonometric parallax distances for Milky Way Cepheids, and eclipsing binary distances for Cepheids in the Large Magellanic Cloud. The H_0 prior was derived

with SN Ia parameters from the MLCS2k2 distance estimator (Jha et al. 2007) given in Hicken et al. (2009b). In principle, for complete consistency with this work, we would use the combined SALT2/SiFTO fits for the same SN events to re-estimate H_0 in a consistent way. However, the maser distance used in Riess et al. (2011) is not published, so we defer this exercise to a future analysis. However, we note that the uncertainty in H_0 given by Riess et al. does include an allowance for the systematic of using SALT2 in place of MLCS2k2 (they quote an increase in H_0 of $1.0 \; \mathrm{km\,s^{-1}\,Mpc^{-1}}$ with SALT2), so most of the systematic difference is likely already included in our error budget.

4. Results

We begin by assessing the magnitude of the various systematic uncertainties in our analysis. For this, we use a simple cosmological model – a flat cosmology with a constant w – and the grid marginalization approach (§ 3).

We then present our main cosmological results. We investigate a non-flat, $w = -1$ cosmology (fitting for Ω_m and Ω_Λ), a flat, constant w cosmology (fitting for Ω_m and w), a non-flat cosmology with w free (fitting for w, Ω_m and Ω_k), and a cosmology where $w(a)$ is allowed to vary via a simple linear parameterization $w(a) = w_0 + w_a(1 - a) \equiv w_0 + w_a z/(1 + z)$ (e.g., Chevallier & Polarski 2001; Linder 2003), fitting for Ω_m, w_0, and w_a. We always fit for α, β, and $\mathcal{M}_B$.

The confidence contours for Ω_m and w in a flat universe can be found in Fig. 1 (upper left panel) for fits considering all systematic and statistical uncertainties. Fig. 1 also shows the statistical-uncertainty-only cosmological fits in the upper right panel. The best-fitting cosmological parameters and the nuisance parameters α, β, $\mathcal{M}_B^1$ and $\mathcal{M}_B^2$, for convenience converted to M_B assuming $H_0 = 70 \, \mathrm{km\,s^{-1}\,Mpc^{-1}}$, are in Table 1 (for non-flat, $w = -1$ fits) and Table 2 (for flat, constant w fits). We also list the parameters obtained with the χ^2 minimization approach for comparison. All the fits, with and without the inclusion of systematic errors, are consistent with a $w = -1$ universe: we find $w = -1.043^{+0.054}_{-0.055}$ (stat), and $w = -1.068^{+0.080}_{-0.082}$ (stat+sys). For comparison, with no external constraints (i.e., SNLS3 only) the equivalent values are $w = -0.90^{+0.16}_{-0.20}$ (stat) and $w = -0.91^{+0.17}_{-0.24}$ (stat+sys) (C11).

The lower right panel of Fig. 1 shows the importance of allowing the nuisance parameters α and β to vary in the fits, rather than holding them fixed at their best-fit values. This leads to not only smaller contours and hence underestimated parameter uncertainties, but also a significant bias in the best-fit parameters (Table 3). Holding α and β fixed gives $w = -1.117^{+0.081}_{-0.082}$, a $\sim 0.6\sigma$ shift in the value of w compared to the correct fit.

The residuals from the best-fitting cosmology as a function of stretch and color can be found in Fig. 2. No significant remaining trends between stretch and Hubble residual are apparent, but there is some evidence for a small trend between SN Ia color and luminosity at $\mathcal{C} < 0.15$ (indicating that these SNe prefer a smaller β, or a shallower slope, than the global value). We examine this,

and related issues, in more detail in § 5.

Covariances between the nuisance parameters are small, with $|r| < 0.15$ for most combinations of α, β and $\mathcal{M}_B$. The exception is between $\mathcal{M}_B^1$ and $\mathcal{M}_B^2$, where the correlation is (as expected) larger ($r \sim 0.6$). Note that this positive covariance enhances the significance of the difference between $\mathcal{M}_B^1$ and $\mathcal{M}_B^2$ beyond the simple statistical uncertainties listed in the tables.

4.1. Systematic error budget

The Ω_m–w flat universe fits (Table 2) represent a 5.2% statistical measurement of w and a 7.6% measure with systematics (i.e., $\simeq 5.5\%$ with systematics only). The total systematic uncertainty is therefore comparable to, but slightly larger than, the statistical uncertainty. The full systematic uncertainty error budget can be found in Table 3. Systematic uncertainties generate about a $\sim 70\%$ increase in the size of the area of the SNLS3+BAO+WMAP7 Ω_m–w 68.3% confidence contour relative to a fit considering statistical errors only (compared to an 85% increase in the SN-only contour; see C11).

The dominant systematic uncertainty is calibration (as in C11), and in particular how well-known the colors and SED of the flux standard (BD $17°$ 4708) are – each of these two terms provides about a 20% increase in the contour area size over the statistical-only fit. The SNLS instrumental zeropoints and filter responses are also a large effect, generating a $\sim 15\%$ increase in each case. In part, this is because the SNLS data are calibrated to the Landolt (1992) system (for comparison to the low-redshift literature SNe), for which the color terms from the SNLS filters are large (Regnault et al. 2009). This situation should improve in the near future as new low redshift SN Ia samples observed in a similar filter system to SNLS become available, dramatically reducing these calibration uncertainties.

By contrast, systematics caused by potential evolution in SN Ia properties (the parameters α and β) are considerably smaller. As discussed in C11, we find no evidence that α varies with redshift, and only marginal evidence for redshift variation in β: explicitly $d\alpha/dz = 0.021 \pm 0.07$ and $d\beta/dz = 0.588 \pm 0.40$ (C11). Is is unlikely that this β evolution is real (G10); however, we conservatively adopt $d\alpha/dz = 0.07$ (the uncertainty in the slope) and $d\beta/dz = 1.0$ in our systematics analysis. Even this amount of redshift evolution in α and β contributes an almost negligible effect (Table 3). The largest identified systematic uncertainty related to the astrophysics of SNe Ia is the implementation of the host-galaxy dependent term in eqn. (2).

The lower left panel of Fig. 1 shows the Ω_m–w contours with all systematics included, *except* those related to calibration. These "no-calibration-systematics" contours are very similar to the statistical-only contours (only a factor 1.07 larger), with $w = -1.048\pm^{+0.057}_{-0.058}$. This represents a total error in w of $\simeq 5.5\%$, and a systematic contribution of $\simeq 1.8\%$, significantly smaller than when the calibration systematics are included. With our current knowledge and fitting techniques for SNe Ia, this represents the systematic floor given a negligible photometric calibration uncertainty.

4.2. Cosmological results

We now present our main cosmological results. We consider various combinations of the SNLS3, WMAP7, SDSS DR7 LRGs, and H_0 datasets: WMAP7+SNLS3+DR7 is the most similar to the constraints used in the grid marginalization approach (Table 2), but still differs as it uses the full matter power spectrum of LRGs rather than the BAO constraint, and the full WMAP7 power spectrum rather than the shift parameters. The best-fitting value of w (Table 4) is therefore slightly different due to these differing external constraints even though the SN Ia constraints are identical, but the percentage error in w is the same at 7.6%.

4.2.1. Constant w fits

All the results are consistent with a spatially flat, $w = -1$ universe. Our results for a flat universe with a constant dark energy equation of state are

$$
\begin{aligned}
\Omega_m &= 0.269 \pm 0.015 \\
w &= -1.061^{+0.069}_{-0.068},
\end{aligned}
$$

and, relaxing the assumption of spatial flatness,

$$
\begin{aligned}
\Omega_m &= 0.271 \pm 0.015 \\
\Omega_k &= -0.002 \pm 0.006 \\
w &= -1.069^{+0.091}_{-0.092},
\end{aligned}
$$

including external constraints from WMAP7 and SDSS DR7 and a prior on H_0 (all quoted uncertainties in this section include both the SN statistical and systematic components). The confidence contours are in Fig. 3 and Fig. 4, and the corresponding best-fit cosmological parameters for various combinations of external constraints can be found in Table 4.

In Table 5 we give a full list of all the best-fit parameters from the constant w `CosmoMC` fits with the WMAP7, SDSS DR7 and H_0 external datasets[3]. This includes some parameters which the SN Ia data do not directly constrain. Ω_b and Ω_c are the fractional energy densities of baryons and dark matter, τ is the reionization optical depth, n_s is the scalar spectral index, A_{05} the amplitude of curvature perturbations at $k = 0.05 \mathrm{Mpc}^{-1}$, and σ_8 the normalization of the matter power spectrum at $8h^{-1}\,\mathrm{Mpc}$.

Of particular note is the high importance of the SN Ia dataset in placing meaningful constraints on w. Assuming a flat universe, WMAP7+DR7 alone only measure w to $\sim$20%, and adding the H_0 prior (i.e., WMAP7+DR7+H_0) only decreases this uncertainty to $\sim$11%. Including the SNLS3

---

[3]Full parameter summaries for all combinations of external datasets can be found at https://tspace.library.utoronto.ca/snls.

dataset with WMAP7+DR7, by contrast, reduces the uncertainty to 7.7%. WMAP7+SNLS3 together also provide a 7.7% measurement. With all external constraints, including the H_0 prior, the measurement of w is 6.5%, comparable to WMAP7+SNLS3 alone.

The situation is slightly different when making no assumption about spatial flatness, but the basic result of the high importance of the SN Ia data remains. In this case, the WMAP7+DR7+SNLS3 data provide an 8.8% measurement, compared to 11.3% without DR7 (the DR7 data make important contributions towards constraining Ω_m). WMAP7+DR7+H_0 alone can only make a $\sim 20\%$ measurement; adding SNLS3 improves this dramatically to $\sim 8.5\%$.

4.2.2. Variable w fits

The final set of fits allow the equation of state parameter w to vary simply as a function of the scale factor, a, as $w(a) = w_0 + w_a(1 - a)$, with a cosmological constant equivalent to $w_0 = -1$, $w_a = 0$. We use a hard prior of $w_0 + w_a \leq 0$, from the constraint of matter domination in the early universe. The confidence contours are in Fig. 5 assuming a flat universe. The best-fit parameters are listed in Table 6. Again, we find no evidence of deviations from the cosmological constant. Assuming a flat universe we find

$$
\begin{aligned}
\Omega_m &= 0.271^{+0.015}_{-0.015} \\
w_0 &= -0.905^{+0.196}_{-0.196} \\
w_a &= -0.984^{+1.094}_{-1.097}.
\end{aligned}
$$

The H_0 prior has only a small effect on the $w(a)$ fits (Fig. 6). As a comparison, with no H_0 prior, we find $w_0 = -0.949^{+0.198}_{-0.201}$, $w_a = -0.535^{+1.109}_{-1.111}$. The SN Ia data are critical for a constraining measurement – without the SN data, fits for w_0 and w_a did not converge.

4.3. Comparison to other results

We compare our results to previous constraints on dark energy using SN Ia data. Komatsu et al. (2011), with a combination of WMAP7, BAO, the Riess et al. (2009) H_0 measurement, plus the Hicken et al. (2009b) SN Ia dataset, found $w_0 = -0.93 \pm 0.13$ and $w_a = -0.41^{+0.72}_{-0.71}$. Although this may appear to be better than our constraints, it did not include a proper handling of SN Ia systematics due to the lack of a consistent, published dataset at that time, and the uncertainties will therefore be under-estimated. Using a slightly larger SN Ia dataset ("Union2") the same WMAP7/BAO constraints, and the Riess et al. (2009) H_0 measurement, Amanullah et al. (2010) find $\Omega_m = 0.274^{+0.016}_{-0.015}$, $\Omega_k = -0.002 \pm 0.007$, and $w = -1.052^{+0.092}_{-0.096}$, comparable to our results (§ 4.2). However, those authors left α and β fixed when computing systematic uncertainties, which may underestimate the size of the final uncertainties (C11, see also Fig. 1 and Table 3), and likely under-estimated the magnitude of the photometric calibration uncertainties (see C11 for discussion).

We also compare our results with those predicted by the Dark Energy Task Force (DETF; Albrecht et al. 2006) for an experiment of this type by calculating the figure of merit (FoM) for our combination of datasets. The exact definition of the FoM has some ambiguity: in the DETF report it is defined as proportional to the reciprocal of the area of the error ellipse in the w_0–w_a plane that encloses 95% of the total probability, but the constant of proportionality is never stated. The values given in Albrecht et al. (2006) are based on performing a transform of variables from w_0 to w_p, the value of w at the so-called pivot redshift z_p, where w_p and w_a are uncorrelated. The FoM is then simply taken to be $1/(\sigma_{w_p}\sigma_{w_a})$. This prescription is the most commonly used in the literature (e.g., Eisenstein et al. 2011), although some authors have been more literal in taking the area of the ellipse. FoM calculations should not assume a flat universe; however current data are poorly constraining without this constraint, so we follow the practice in the literature and assume flatness in our FoM numbers.

For our WMAP7+DR7+SNLS3+H_0 fit in a flat universe, we find $z_p \simeq 0.19$ and $w_p = -1.063 \pm 0.082$. Combined with our measurement of w_a, we find a FoM of 11.1 (see also Table 6). Excluding the SHOES H_0 prior gives a FoM of 10.6. Directly taking the reciprocal of the area of the 95% confidence intervals give 0.56 and 0.44 respectively.

In DETF terminology, the SNLS3 sample represents a stage II SN experiment, and the final combination of this and other stage II experiments is predicted to give a FoM of $\simeq 50$. However, these figures are difficult to compare with our results. The DETF calculations assume a far larger SN Ia sample of 1200 events (including, significantly, 500 at low-redshift), together with a (superior) CMB prior from the Planck satellite (Planck Collaboration et al. 2011) rather than WMAP, and also include cluster and weak lensing experiments. They do not include BAO or H_0 information, although the latter only has a small effect on the FoM.

5. Supernova sub-samples

A complementary approach to checking and analyzing systematics, in particular those that are not susceptible to an analytical approach, is to break the SN Ia sample into sub-samples which probe either different experimental systematics, or different regions of parameter space of the SN Ia population. For example, the stretch–luminosity and color–luminosity relations are assumed to be linear, universal and invariant with (e.g.) SN properties, and the size of the SNLS3 sample allows us to test these assumptions in detail. Furthermore, the cosmological results should be robust to any segregation of the data if the systematics are handled correctly.

For simplicity, we use the χ^2 minimization approach in this section. We first split the SNLS SNe according to location on the sky (i.e., one of the four CFHT-LS deep fields). We then test the robustness of the nuisance parameters by splitting the sample by SN and their host galaxy parameters.

5.1. Segregation by SNLS field

We first test for any variations in w as a function of the field in which the SNLS SN occurred. SNLS observes in four fields distributed in right ascension (see Sullivan et al. 2006a, for the field coordinates), so we can test for a combination of photometric calibration systematics, as well as a physically varying w in different directions, by comparing the cosmological parameters we derive from each field. To do this, we adjust our χ^2 minimization approach to fit for global nuisance parameters (α, β, and $\mathcal{M}_B$) for all SNe, but with a different w and Ω_m in each of the four different SNLS fields. The average w and Ω_m for the four fields is applied to the external SNe and for combination with WMAP7 and the BAO constraints.

This approach effectively adds six new terms to the fit. The results can be found in Table 7. The χ^2 only drops from 418.1 (for 466 DOF) to 414.9 (for 460 DOF), indicating that the fields are consistent. Comparing the individual field Ω_m and w values to the average values of the four fields, and allowing for the covariances between the individual values, gives a χ^2 of 3.38 for 6 DOF, consistent with the χ^2 distribution and indicating no significant variability among the different fields.

5.2. Segregation by SN properties

The SN Ia light curve shape is well-known to vary systematically as a function of the SN environment. Fainter SNe Ia with faster light curves are preferentially located in older stellar populations, while the brighter examples with broad light curves tend to explode in late-type spiral or star-forming systems (e.g., Hamuy et al. 1995, 2000; Sullivan et al. 2006b). When coupled with the evidence for both a young and old component to the SN Ia progenitor population (Mannucci et al. 2005, 2006; Sullivan et al. 2006b; Brandt et al. 2010), or at least a wide-range in the SN delay-times (Pritchet et al. 2008; Totani et al. 2008), a natural prediction is a subtle change in the mix of SN light curve shapes with redshift (Howell et al. 2007).

If the stretch–luminosity relation is universal across SN stretch and progenitor age, this predicted drift will not impact the determination of the cosmological parameters – a low-stretch SN should correct equally well as a high-stretch SN. To test this, we split our SN sample into two groups ($s<1$ and $s\geq1$) and perform independent cosmological fits to each sub-sample. This obviously restricts the lever-arm in stretch and so the α coefficient is less well-determined; nonetheless this is a useful test of the utility of SNe Ia across different environments.

When considering sub-samples of SNe classified by SN properties (for example stretch or color), the Malmquist corrections that are applied globally to the sample will not be appropriate. For example, low stretch SNe Ia are intrinsically fainter and will suffer from a larger selection effect at high-redshift than high stretch events. Rather than apply different Malmquist corrections for these different sub-samples (which could in principle be derived from simulations such as those

in Perrett et al. 2010), we instead restrict the SNe to the redshift ranges over which selection effects are reduced. For the SNLS sample, we restrict to $z < 0.75$, and for the SDSS sample, we restrict to $z < 0.3$. These data also tend to be better observed, being brighter, with smaller error bars on the SN parameters. We also discard the small HST sample. We perform both statistical and statistical+systematic uncertainty fits – the comparison is useful as we are interested in the differences between SN Ia sub-samples, and many of systematics affect sub-samples in a similar way.

The results are given in Table 8 and Fig. 7, the latter generated from the covariance matrices of the fits.. The derived cosmological parameters are consistent between low and high-s SNe Ia, although the nuisance parameters show some differences: the α values are consistent between low-s and high-s, but much larger than the full sample. The M_B values show large differences between low-s and high-s. However, there are significant (and expected) covariances between α and M_B in these fits: for the low-s group, M_B^1 increases as α decreases, while for the high-s group M_B^1 decreases for decreasing α (and a similar trend is seen for M_B^2). As M_B is defined at $s = 1$, which the SNe in neither group sample, the two parameters become quite inter-dependent. When considering the joint confidence contours between α, M_B^1, and M_B^2 (Fig. 7) only mild tensions are seen. A slightly larger tension is seen in the value of β for the two sub-groups: the values 2.90 ± 0.16 and 3.25 ± 0.14 differ at $\sim 2.2\sigma$ (Table 8).

In a similar vein, we also split the sample by SN color at $\mathcal{C} = 0$. Unlike stretch, SN color (examined independently of SN luminosity) shows no clear evidence for variation with environment. No robust trends have been found despite rigorous examinations (e.g., Sullivan et al. 2010; Lampeitl et al. 2010), and we also find no significant trends of the nuisance parameters varying as a function of SN color.

5.3. Segregation by host galaxy characteristics

We also segregate the SNLS3 sample according to the environment in which the SN exploded. This is a fundamentally different test, dividing the sample according to the environment of the SN rather than its direct properties (although significant correlations exist between, for example, SN stretch and host galaxy M_{stellar} or star-formation rate). For these tests we use M_{stellar} to segregate the sample, as used in the cosmological fits, following Sullivan et al. (2010). As we already use a different M_B for SNe Ia in low and high M_{stellar} galaxies in our standard fits, we simply adapt this approach to additionally fit for a different α and β in the two host classes. This has the advantage that we are no longer comparing the results of different fits as we fit for all the nuisance parameters simultaneously, and we can use the full systematics covariance matrix, as well as the full SN Ia sample. (We also provide the fit results when we physically divide the sample into two, for comparison with § 5.2, in Table 8.) Note that in these fits we do not include the host galaxy systematic term, as we are trying to examine the effect of any host galaxy dependence.

The "multi nuisance parameter" fit results are shown in Table 9, which gives the values of the nuisance parameters themselves, and Table 10, which gives the effect on w and the χ^2. The joint confidence contours for some of the nuisance parameters are shown in Fig. 8. For completeness, we also give results when only one M_B is used.

The data do not support the addition of a different α parameter in low and high mass galaxies – when this is added to the fits, the α values are generally consistent and the quality of the fit, as indicated by the χ^2, is unchanged. This is true even when only one M_B is used in the fits, and suggests that α is fairly insensitive to the details of the environment and characteristics of the SN Ia progenitor stellar population.

However, there is evidence for different M_B (as already fit for) and different β. The value of β is ~ 3.7 in low mass galaxies, versus ~ 2.8 in high-mass galaxies, regardless of whether two M_B are used. A similar trend is seen when physically dividing the sample into two and performing separate independent fits as in the previous section (Table 8), and is consistent with the β difference seen between low and high-stretch SNe in § 5.2, as low-stretch SNe are preferentially found in massive host galaxies. Generally, the two β values show only a very small positive covariance, and differ at the $\sim 4.3\sigma$ level. There is also a substantial reduction in the χ^2 of the fit when including two β terms. For example, fitting for two βs and two M_B reduces the χ^2 to 405.4 from the 423.1 obtained if only one β is used (for 465 and 466 DOF). An F-test indicates that this additional term is required at $\simeq 4.5\sigma$.

The variation of β with host properties has been observed at lower significance by Sullivan et al. (2010) in the SNLS sample, and by Lampeitl et al. (2010) in the SDSS SN Ia sample (a larger SDSS SN Ia sample than the one used in this paper). Lampeitl et al. (2010) find $\beta \sim 2.5$ in passive host galaxies, and $\beta \sim 3.1$ in star-forming host galaxies. Using their full sample, the significance is $\sim 3.5\sigma$, although this drops to $< 2\sigma$ when considering only cosmologically useful events with normal stretches and colors using similar cuts to those used in this paper.

5.4. Discussion

The most significant result from our analysis of the SN sub-samples is the additional variation of β, as well as M_B, between low- and high-M_{stellar} host galaxies. This effect appears real in our data and so should be accounted for appropriately in our cosmological results. We therefore examine the systematic effect of *not* including this term, and compare to our existing systematic uncertainty error budget.

Compared to a statistical uncertainty only fit, the addition of two αs and two βs, gives a $\Delta\Omega_m = 0.00$ and $\Delta w = 0.005$ (Table 10). The mean statistical-only errors on Ω_m and w are 0.0148 and 0.0545 (Table 3). Adding in quadrature the shifts measured when including the two αs and βs increases the w uncertainty to 0.0547. This total uncertainty on w is smaller than the uncertainty obtained when including host galaxy systematic term listed in (0.0559; Table 3), i.e. the effect on

w of introducing two βs is smaller than our current host galaxy systematic term.

Note this would not be the case if we had neglected all nuisance parameter variation, i.e. had only used one M_B in our cosmological fits. In this case, $\Delta\Omega_m = 0.005$ and $\Delta w = 0.055$ (the shift from considering one M_B to considering two M_B); in the case of w this is a shift larger than our statistical uncertainty, and is comparable to our total systematic uncertainty, becoming the dominant term in the error budget. Thus while the use of different M_B is essential for a SN Ia cosmological analysis, the use of two βs *and* two M_Bs is not. Note that no previous SN Ia cosmological analysis has performed this host galaxy correction, indicating that systematic uncertainties will be significantly under-estimated in these studies.

A similar argument can be made using the fits including systematic uncertainties. Here, we compare fits that do include the host galaxy systematic term (unlike the numbers in Table 10), as we wish to examine whether the size of any shift in the cosmological parameters with the addition of two βs is accounted for by our existing systematic uncertainty error budget. In this case, $\Delta w = 0.015$. Our total error in w is 0.0810, compared to 0.0800 excluding the host systematic term (see Table 3). Adding the 0.015 in quadrature to this 0.0800 gives a w uncertainty of 0.0813, a total uncertainty on w almost the same as that obtained when using the host systematic term. Therefore, our conclusion is that while the two β effect appears real in our data, it is adequately accounted for by our systematic uncertainty error budget.

Although the variation of β with host parameters is not a concern for this cosmological analysis, it does have implications for the physical origin of color variation in SNe Ia which may impact future surveys. A long-standing observation is that the slope of the relation between M_B and $B - V$ (i.e., β) is $\ll 4.1$ (Tripp 1998; Astier et al. 2006), the value expected based on Milky Way like dust if β is interpreted as the ratio of total-to-selective extinction R_B (where $R_B \equiv R_V + 1$, and $R_V \simeq 3.1$ for the Milky Way). The effective β for SNe Ia is likely a conflation of different physical effects, including extinction by dust (which may vary with host type, e.g., Lampeitl et al. 2010; Sullivan et al. 2010, and this paper) and intrinsic variation in SN color that does not correlate with SN light curve shape (e.g., Folatelli et al. 2010), and which may depend on variables such as explosion asymmetry or observational viewing angle (Kasen et al. 2009; Maeda et al. 2011). Recent work has shown that SN color is also correlated with SN Ia spectral features, with SNe possessing faster ejecta velocities having redder colors at fixed M_B (or equivalently brighter M_B at fixed color) in samples with very red SNe excluded (Foley & Kasen 2011).

Under the assumption that any intrinsic SN Ia color–luminosity relation has a smaller effective β than that from dust (as seems likely given we observe $\beta < 4.1$), our results are qualitatively consistent with a scenario in which dust extinction modifies this intrinsic color–luminosity relation. The lowest $M_{stellar}$ host galaxies are those with the largest specific SFRs, and therefore the largest dust content. We would therefore expect to find SNe Ia with a larger effective β (i.e., closer to the true dust value) in lower $M_{stellar}$ hosts, which is consistent with our observations. In more massive, passive host galaxies, we are likely observing a β closer to the intrinsic value.

6. Conclusions

In this paper we have presented the cosmological results for the Supernova Legacy Survey (SNLS) three-year SN Ia sample (SNLS3; G10; C11), combined with other constraints from the literature. Our SN Ia sample contains 472 SNe, including 242 from SNLS (G10), 123 at low redshift, 93 from SDSS-SN, and 14 from HST (see C11). We have performed analyses investigating the cosmological parameters Ω_m, Ω_k, and the dark energy equation-of-state parameter w. A key aspect of our analysis is the inclusion of all identified SN Ia systematic uncertainties directly in our cosmological fits (C11). The inclusion of these systematic uncertainties has two key effects. Foremost, the uncertainties that we quote on the cosmological parameters reflect the systematic component. Second, correlations in brightness, stretch and color between different SNe due to their being affected by the same systematic are accounted for during the cosmological fitting stage. We also correct for recently identified trends between SN Ia brightness and host galaxy stellar mass.

Our main results are:

1. For simple cosmological fits assuming a flat Universe and constant w, combining the SNLS3 sample with BAO observations and the WMAP7 CMB "shift" parameters gives $\Omega_m = 0.276^{+0.016}_{-0.013}$ and $w = -1.043^{+0.054}_{-0.055}$, where the error is statistical only. When we include all identified SN Ia systematics in the fits, we find $\Omega_m = 0.274^{+0.019}_{-0.015}$ and $w = -1.068^{+0.080}_{-0.082}$.

2. In terms of the contribution towards the uncertainty in measuring w in the above fits, our systematic and statistical uncertainties are approximately equal (5.5% and 5.2% respectively). However, the systematic uncertainty error budget is dominated by the photometric calibration of the SN fluxes, rather than uncertainties related to the astrophysics of the SNe themselves. Neglecting calibration uncertainties, likely to be dramatically reduced in the future, gives a systematic uncertainty of $\sim 2\%$.

3. When including the SHOES prior on H_0, together with the full WMAP7 power spectrum and the power spectrum of LRGs in SDSS DR7, we find $\Omega_m = 0.269 \pm 0.015$ and $w = -1.061^{+0.069}_{-0.068}$ using the `CosmoMC` fitter, a 6.5% measure of w. When we relax the assumption of a flat Universe, we find $\Omega_m = 0.271 \pm 0.015$, $\Omega_k = -0.002 \pm 0.006$, and $w = -1.069^{+0.091}_{-0.092}$. These include all SN systematic uncertainties.

4. We consider a simple parameterization of the time variation of w as $w(a) = w_0 + w_a(1 - a)$. Assuming a flat Universe we find $\Omega_m = 0.271^{+0.015}_{-0.015}$, $w_0 = -0.905^{+0.196}_{-0.196}$ and $w_a = -0.984^{+1.094}_{-1.097}$. This includes WMAP7, SDSS-DR7, and the SHOES H_0 prior as external constraints. Our results are equivalent to a DETF figure-of-merit of ~ 11.

5. We investigate astrophysical systematics in our SN Ia sample by breaking it into sub-samples based on SN light curve and host galaxy parameters. Cosmologies determined from these SN sub-samples are fully consistent. However, we find significant evidence (4.4σ) for a different β between low and high stellar mass host galaxies (as well as a different M_B, which we already

account for). The effect of this varying β on the cosmology lies well within the current systematic uncertainty assigned to host-galaxy-dependent corrections, but our analysis emphasizes the critical need to make host galaxy related corrections when determining the cosmological parameters.

When the SNLS3 sample is combined with measurements of large scale structure, observations of the CMB, and a prior on H_0, the constraints on dark energy presented here are the tightest available, and the only ones that directly include all identified SN Ia systematic uncertainties in the analysis. All our results are consistent with a flat, $w = -1$ universe.

The primary contributor to the systematic error budget is the calibration of the SN Ia fluxes, both placing them on a consistent system between different SN Ia surveys, and then interpreting that system when fitting the SN light curves. The magnitude of the identified astrophysical systematics is significantly smaller than calibration related uncertainties. Those that have been uncovered in the SN Ia population can be adequately controlled using empirical corrections based on the properties of the SN Ia host galaxies.

The implication is that, if the calibration-related systematics can be reduced, SNe Ia are a long way from being systematics limited. In part, the calibration-related systematics arise from the need to calibrate the $griz$ SNLS and SDSS filter sets to the $UBVR$ system used for the majority of the low-redshift SN Ia data. This situation is set to improve considerably as improved low redshift SN Ia samples become available (e.g., Keller et al. 2007; Law et al. 2009). These new samples will be directly calibrated to the SNLS system (or vice-versa) and will eliminate, or at least substantially reduce, the main systematic uncertainties, allowing the full potential of the SNLS sample to be unlocked.

REFERENCES

Albrecht, A., et al. 2006, ArXiv Astrophysics e-prints

Amanullah, R., et al. 2010, ApJ, 716, 712

Astier, P., et al. 2006, A&A, 447, 31

Balland, C., et al. 2009, A&A, 507, 85

Bazin, G., et al. 2011, in A&A, submitted

Bennett, C. L., et al. 2003, ApJS, 148, 1

Blondin, S., et al. 2006, AJ, 131, 1648

Brandt, T. D., Tojeiro, R., Aubourg, É., Heavens, A., Jimenez, R., & Strauss, M. A. 2010, AJ, 140, 804

Bronder, T. J., et al. 2008, A&A, 477, 717

Chevallier, M., & Polarski, D. 2001, International Journal of Modern Physics D, 10, 213

Cole, S., et al. 2005, MNRAS, 362, 505

Conley, A., Carlberg, R. G., Guy, J., Howell, D. A., Jha, S., Riess, A. G., & Sullivan, M. 2007, ApJ, 664, L13

Conley, A., et al. 2011, ApJS, 192, 1

Conley, A., et al. 2008, ApJ, 681, 482

Contreras, C., et al. 2010, AJ, 139, 519

Cooke, J., et al. 2011, ApJ, 727, L35+

Copeland, E. J., Sami, M., & Tsujikawa, S. 2006, International Journal of Modern Physics D, 15, 1753

de Bernardis, P., et al. 2002, ApJ, 564, 559

Eisenstein, D. J., et al. 2011, ArXiv e-prints

Eisenstein, D. J., et al. 2005, ApJ, 633, 560

Ellis, R. S., et al. 2008, ApJ, 674, 51

Fang, W., Hu, W., & Lewis, A. 2008, Phys. Rev. D, 78, 087303

Folatelli, G., et al. 2010, AJ, 139, 120

Foley, R. J., et al. 2008, ApJ, 684, 68

Foley, R. J., & Kasen, D. 2011, ApJ, 729, 55

Frieman, J. A., Turner, M. S., & Huterer, D. 2008, ARA&A, 46, 385

Guy, J., et al. 2007, A&A, 466, 11

Guy, J., et al. 2010, A&A, 523, A7+

Hamuy, M., Phillips, M. M., Maza, J., Suntzeff, N. B., Schommer, R. A., & Aviles, R. 1995, AJ, 109, 1

Hamuy, M., et al. 1996, AJ, 112, 2408

Hamuy, M., Trager, S. C., Pinto, P. A., Phillips, M. M., Schommer, R. A., Ivanov, V., & Suntzeff, N. B. 2000, AJ, 120, 1479

Hicken, M., et al. 2009a, ApJ, 700, 331

Hicken, M., Wood-Vasey, W. M., Blondin, S., Challis, P., Jha, S., Kelly, P. L., Rest, A., & Kirshner, R. P. 2009b, ApJ, 700, 1097

Hillebrandt, W., & Niemeyer, J. C. 2000, ARA&A, 38, 191

Holtzman, J. A., et al. 2008, AJ, 136, 2306

Hook, I. M., et al. 2005, AJ, 130, 2788

Howell, D. A. 2010, ArXiv e-prints

Howell, D. A., Sullivan, M., Conley, A., & Carlberg, R. 2007, ApJ, 667, L37

Howell, D. A., et al. 2005, ApJ, 634, 1190

Hsiao, E. Y., Conley, A., Howell, D. A., Sullivan, M., Pritchet, C. J., Carlberg, R. G., Nugent, P. E., & Phillips, M. M. 2007, ApJ, 663, 1187

Jha, S., et al. 2006, AJ, 131, 527

Jha, S., Riess, A. G., & Kirshner, R. P. 2007, ApJ, 659, 122

Jönsson, J., et al. 2010, MNRAS, 405, 535

Kasen, D., Röpke, F. K., & Woosley, S. E. 2009, Nature, 460, 869

Keller, S. C., et al. 2007, Publications of the Astronomical Society of Australia, 24, 1

Kelly, P. L., Hicken, M., Burke, D. L., Mandel, K. S., & Kirshner, R. P. 2010, ApJ, 715, 743

Kessler, R., et al. 2010, PASP, 122, 1415

Kessler, R., et al. 2009, ApJS, 185, 32

Komatsu, E., et al. 2009, ApJS, 180, 330

Komatsu, E., et al. 2011, ApJS, 192, 18

Krueger, B. K., Jackson, A. P., Townsley, D. M., Calder, A. C., Brown, E. F., & Timmes, F. X. 2010, ApJ, 719, L5

Lampeitl, H., et al. 2010, ApJ, 722, 566

Landolt, A. U. 1992, AJ, 104, 340

Larson, D., et al. 2011, ApJS, 192, 16

Law, N. M., et al. 2009, PASP, 121, 1395

Le Borgne, D., & Rocca-Volmerange, B. 2002, A&A, 386, 446

Lewis, A., & Bridle, S. 2002, Phys. Rev. D, 66, 103511

Linder, E. V. 2003, Physical Review Letters, 90, 091301

Maeda, K., et al. 2011, ArXiv e-prints

Mannucci, F., Della Valle, M., & Panagia, N. 2006, MNRAS, 370, 773

Mannucci, F., della Valle, M., Panagia, N., Cappellaro, E., Cresci, G., Maiolino, R., Petrosian, A., & Turatto, M. 2005, A&A, 433, 807

Miknaitis, G., et al. 2007, ApJ, 666, 674

Percival, W. J., et al. 2007, ApJ, 657, 51

Percival, W. J., et al. 2010, MNRAS, 401, 2148

Perlmutter, S., et al. 1999, ApJ, 517, 565

Perrett, K., et al. 2010, AJ, 140, 518

Phillips, M. M. 1993, ApJ, 413, L105

Planck Collaboration, et al. 2011, ArXiv e-prints

Pritchet, C. J., Howell, D. A., & Sullivan, M. 2008, ApJ, 683, L25

Regnault, N., et al. 2009, A&A, 506, 999

Reid, B. A., et al. 2010, MNRAS, 404, 60

Riess, A. G., et al. 1998, AJ, 116, 1009

Riess, A. G., et al. 1999, AJ, 117, 707

Riess, A. G., et al. 2011, ApJ, 730, 119

Riess, A. G., et al. 2009, ApJ, 699, 539

Riess, A. G., Press, W. H., & Kirshner, R. P. 1996, ApJ, 473, 88

Riess, A. G., et al. 2007, ApJ, 659, 98

Schlegel, D. J., Finkbeiner, D. P., & Davis, M. 1998, ApJ, 500, 525

Sullivan, M., et al. 2010, MNRAS, 406, 782

Sullivan, M., Ellis, R. S., Howell, D. A., Riess, A., Nugent, P. E., & Gal-Yam, A. 2009, ApJ, 693, L76

Sullivan, M., et al. 2006a, AJ, 131, 960

Sullivan, M., et al. 2006b, ApJ, 648, 868

Totani, T., Morokuma, T., Oda, T., Doi, M., & Yasuda, N. 2008, PASJ, 60, 1327

Tripp, R. 1998, A&A, 331, 815

Walker, E. S., et al. 2011, MNRAS, 410, 1262
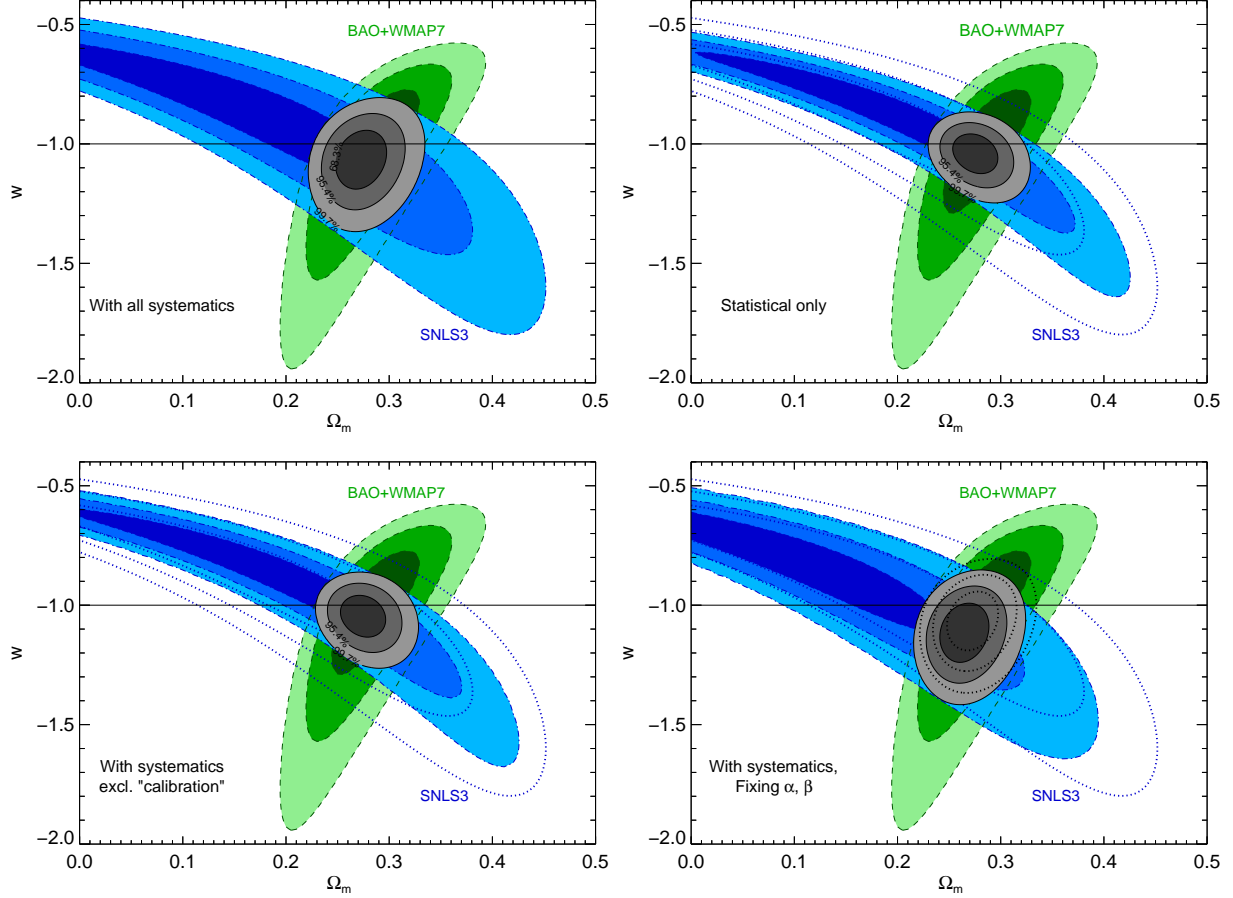
Fig. 1.— Confidence contours in the cosmological parameters Ω_m and w arising from fits to the combined SN Ia sample using the marginalization fitting approach, illustrating various systematic effects in the cosmological fits. In all panels, the SNLS3 SN Ia contours are shown in blue, and combined BAO/WMAP7 constraints (Percival et al. 2010; Komatsu et al. 2011) in green. The combined constraints are shown in grey. The contours enclose 68.3%, 95.4% and 99.7% of the probability, and the horizontal line shows the value of the cosmological constant, $w = -1$. Upper left: The baseline fit, where the SNLS3 contours include statistical and all identified systematic uncertainties. Upper right: The filled SNLS3 contours include statistical uncertainties only; the dotted open contours refer to the baseline fit with all systematics included. Lower left: The filled SNLS3 contours exclude the SN Ia systematic uncertainties related to calibration. Lower right: The filled SNLS3 contours result from fixing α and β in the cosmological fits. See Table 2 and Table 3 for numerical data.
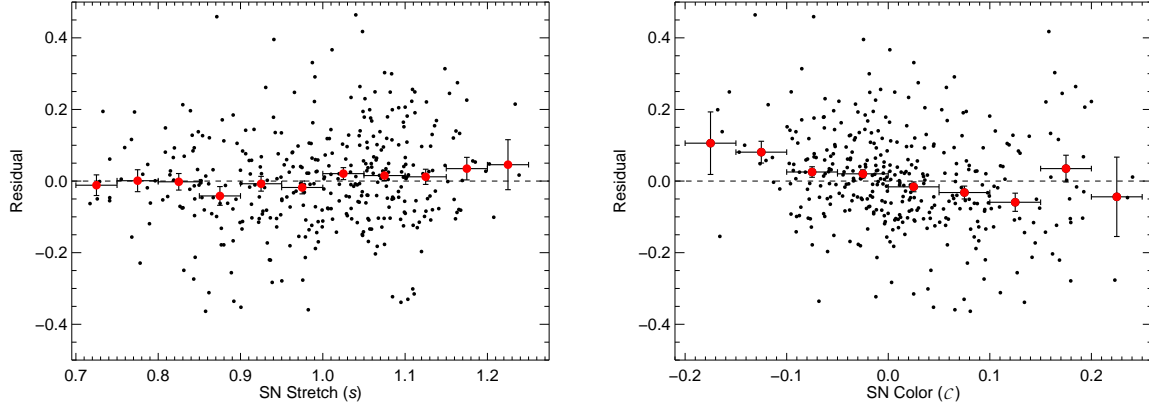
Fig. 2.— Residuals (in magnitudes) from the best-fitting flat cosmology as a function of stretch (left) and color (right). Residuals are defined as $m_B - m_B^{\mathrm{mod}}$, i.e., negative residuals indicate brighter SNe (after application of stretch– and color–luminosity relations). Red points show the mean residuals in bins of stretch and color. The dashed line indicates a zero residual.
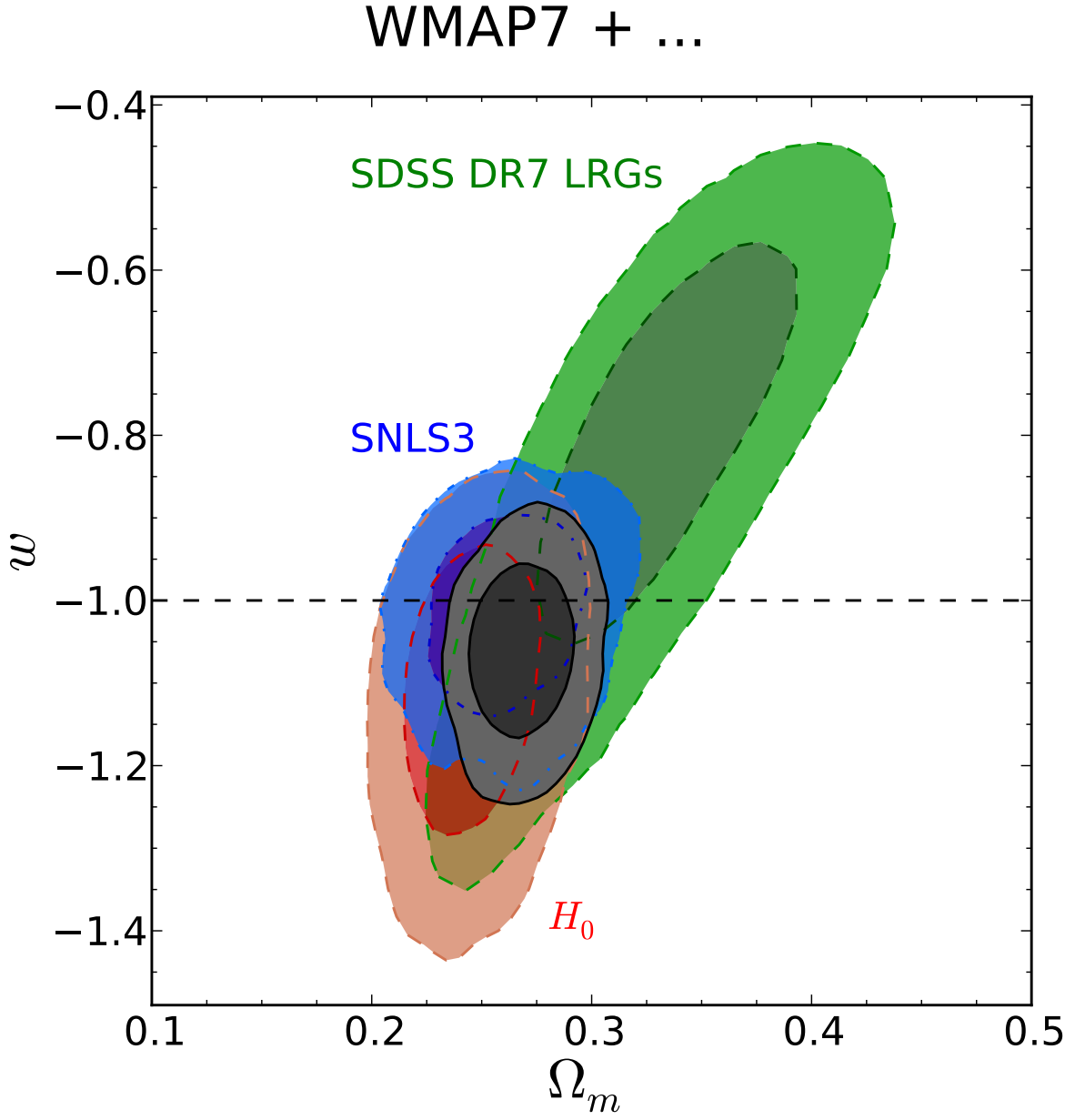
Fig. 3.— Confidence contours in the cosmological parameters Ω_m and w assuming a flat universe, produced using the `CosmoMC` program. The SNLS3 contours are in blue, the SDSS DR7 LRG contours in green, and the H_0 prior in red. WMAP7 constraints are included in all contours. The contours enclose 68.3% and 95.4% of the probability and include all SN systematic uncertainties. The dashed line indicates $w = -1$. Numerical results are in Table 4.
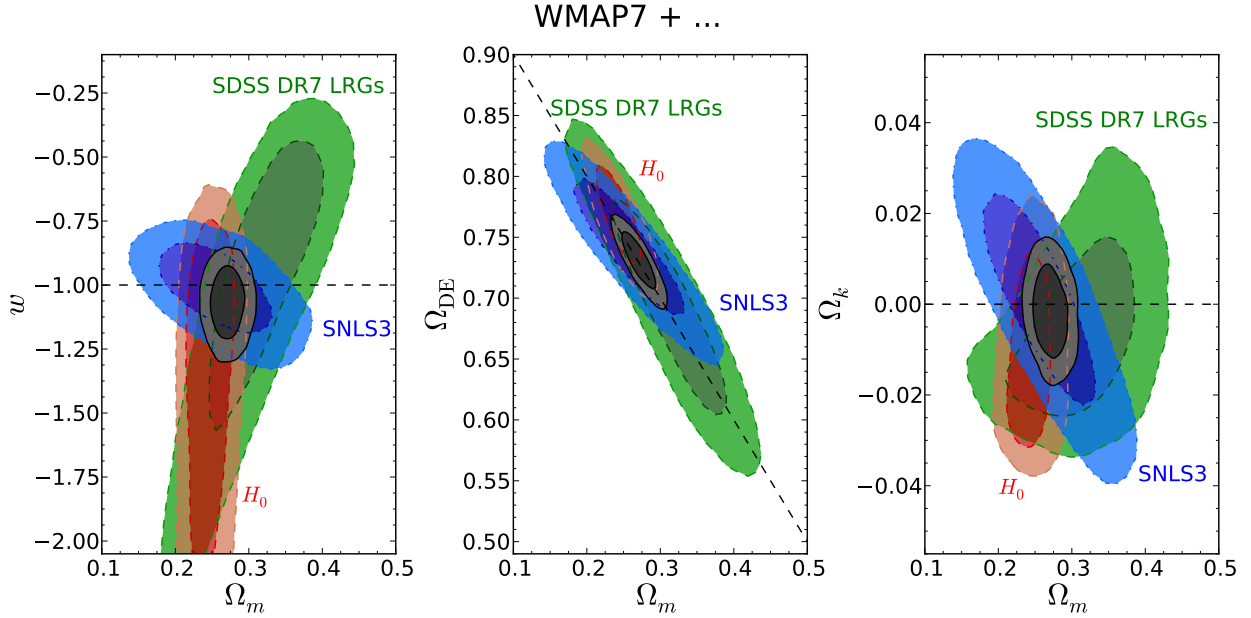
Fig. 4.— Confidence contours in the cosmological parameters Ω_m, Ω_{DE}, Ω_k, and w produced using the CosmoMC program. The SNLS3 contours are in blue, the SDSS DR7 LRG contours in green, and the H_0 prior in red. WMAP7 constraints are included in all contours. The contours enclose 68.3% and 95.4% of the probability and include all SN systematic uncertainties. In the left-hand panel, the dashed line indicated $w = -1$; in the center and right-hand panels the line indicates a flat ($\Omega_k = 0$) universe. Numerical results are in Table 4.
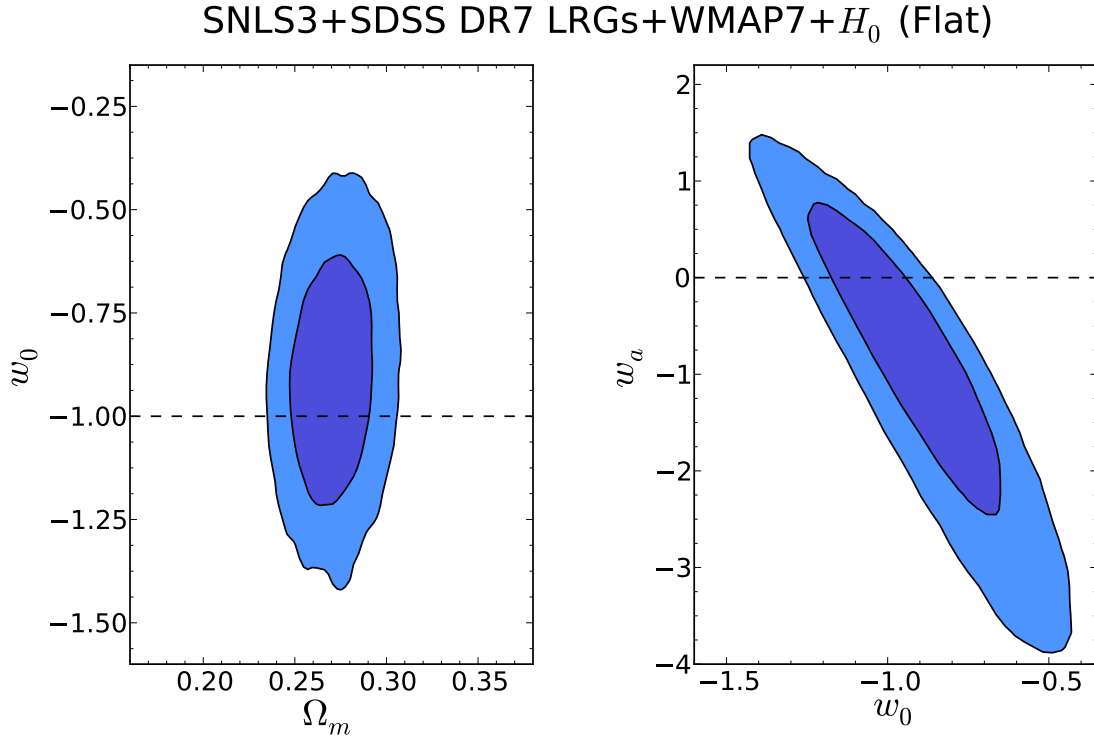
Fig. 5.— Combined confidence contours in Ω_m, w_0, and w_a using SNLS3, WMAP7, SDSS DR7 LRGs, and a prior on H_0. A flat universe is assumed. The horizontal dashed lines indicate a cosmological constant ($w_0 = -1$; left) and a non-varying w ($w_a = 0$; right). All SN Ia systematic uncertainties are included. Numerical results are in Table 6.
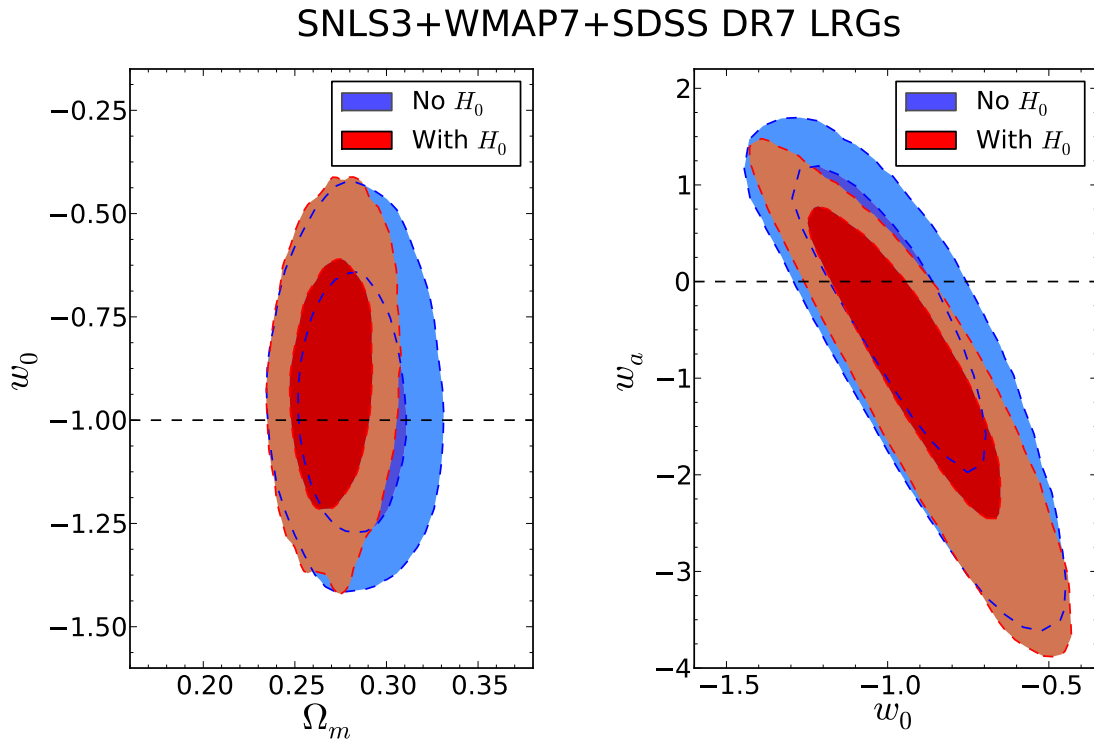
Fig. 6.— The effect of the H_0 prior on the Ω_m, w_0, and w_a contours in a flat universe. The red contours show the fits with the H_0 prior, and the blue contours without.
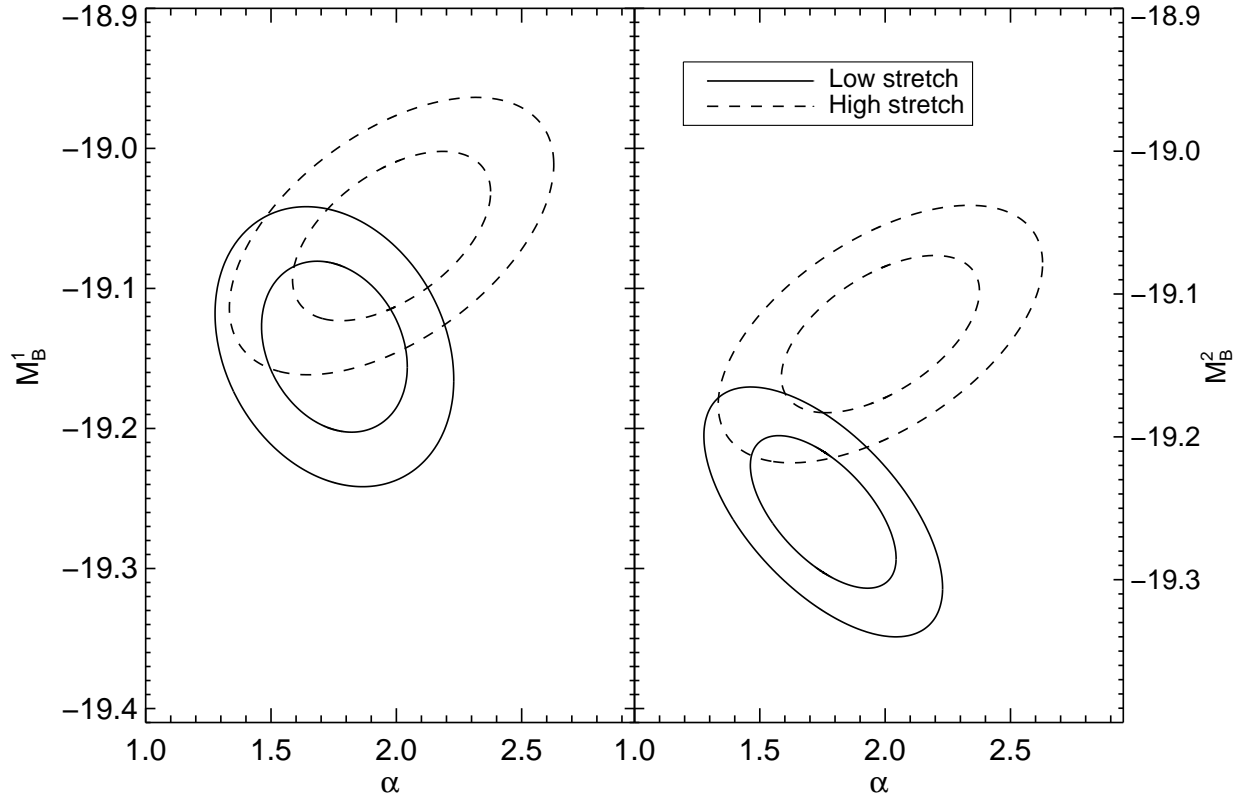
Fig. 7.— Joint confidence contours between the nuisance parameters α, M_B^1 (left), and M_B^2 (right) for low-stretch (solid line) and high-stretch (dashed line) SNe Ia, using the restricted SN Ia sample described in § 5.2. The contours enclose 68.3% and 95.4% of the probability, and the fits include all systematic uncertainties. Only mild tensions exist.
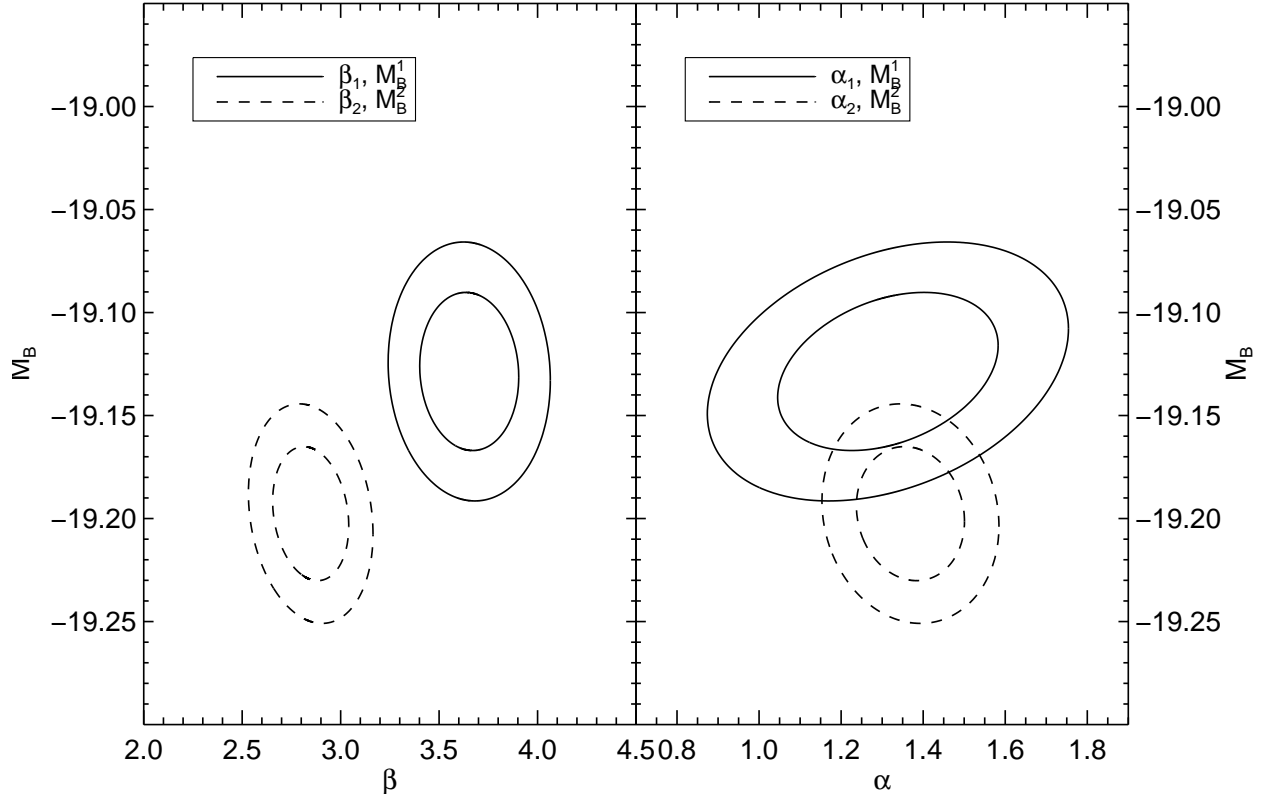
Fig. 8.— Joint confidence contours in the nuisance parameters β and M_B (left) and α and M_B (right), allowing all the nuisance parameters to vary according to host galaxy stellar mass. $\alpha_1/\beta_1/M_B^1$ refer to SNe Ia in hosts with $M_{\rm stellar} \leq 10^{10} M_\odot$, and $\alpha_2/\beta_2/M_B^2$ to SNe Ia in hosts with $M_{\rm stellar} > 10^{10} M_\odot$. The full SNLS3 sample is used, and all systematic uncertainties are included. A significant variation in β with host $M_{\rm stellar}$ is observed.

Table 1.   Cosmological results assuming $w = -1$ for the SNLS3 sample plus BAO[b] and WMAP7[c]

Fit	α	β	$M_B^{1\,\text{a}}$	$M_B^{2\,\text{a}}$	Ω_m	Ω_Λ
			Marginalization fits			
Stat only	$1.451^{+0.123}_{-0.100}$	$3.165^{+0.105}_{-0.089}$	-19.122	-19.198	$0.275^{+0.016}_{-0.013}$	$0.727^{+0.015}_{-0.013}$
Stat + sys	$1.428^{+0.121}_{-0.098}$	$3.263^{+0.121}_{-0.103}$	-19.144	-19.196	$0.279^{+0.019}_{-0.015}$	$0.724^{+0.017}_{-0.016}$
			χ^2 minimization fits			
Stat only	$1.389^{+0.085}_{-0.083}$	$3.144^{+0.095}_{-0.092}$	$-19.121^{+0.015}_{-0.015}$	$-19.196^{+0.013}_{-0.013}$	$0.273^{+0.015}_{-0.014}$	$0.729^{+0.014}_{-0.014}$
Stat + sys	$1.368^{+0.086}_{-0.084}$	$3.182^{+0.102}_{-0.099}$	$-19.162^{+0.028}_{-0.029}$	$-19.206^{+0.024}_{-0.024}$	$0.274^{+0.017}_{-0.016}$	$0.732^{+0.016}_{-0.017}$

[a]For an $s = 1$ and $\mathcal{C} = 0$ SN Ia. Computed from $\mathcal{M}_B$ (§ 3) assuming $H_0 = 70\,\text{km s}^{-1}\,\text{Mpc}^{-1}$. Errors on $\mathcal{M}_B$ are not available in the marginalization (grid) approach as the variable is analytically marginalized; the quoted value is an estimate only.

[b]Percival et al. (2010)

[c]Using the WMAP7 "shift" parameter R, the "acoustic scale" l_a, and the decoupling redshift z_* from Komatsu et al. (2011)

Table 2.   Cosmological results assuming a flat universe and constant w for the SNLS3 sample
plus BAO and WMAP7

Fit	α^{a}	β^{a}	M_B^1	M_B^2	Ω_m	w
			Marginalization fits			
Stat only	$1.450^{+0.112}_{-0.105}$	$3.164^{+0.096}_{-0.094}$	-19.164	-19.227	$0.276^{+0.016}_{-0.013}$	$-1.043^{+0.054}_{-0.055}$
Stat + sys	$1.367^{+0.086}_{-0.084}$	$3.179^{+0.101}_{-0.099}$	-19.175	-19.220	$0.274^{+0.019}_{-0.015}$	$-1.068^{+0.080}_{-0.082}$
			χ^2 minimization fits			
Stat only	$1.395^{+0.085}_{-0.083}$	$3.148^{+0.095}_{-0.092}$	$-19.130^{+0.019}_{-0.019}$	$-19.203^{+0.016}_{-0.016}$	$0.274^{+0.015}_{-0.014}$	$-1.039^{+0.052}_{-0.055}$
Stat + sys	$1.367^{+0.086}_{-0.084}$	$3.179^{+0.101}_{-0.099}$	$-19.155^{+0.027}_{-0.027}$	$-19.200^{+0.023}_{-0.023}$	$0.272^{+0.017}_{-0.016}$	$-1.058^{+0.078}_{-0.082}$

[a]Note that the values of these nuisance parameters differ very slightly from those from the SN-only fits given in C11 due to small correlations between the cosmological parameters and the nuisance parameters.

Table 3. Detailed summary of systematic uncertainties

Source	Ω_m	w	Relative area[a]
Statistical only	$0.2763^{+0.0163}_{-0.0132}$	$-1.0430^{+0.0543}_{-0.0546}$	1.0
All systematics	$0.2736^{+0.0186}_{-0.0145}$	$-1.0676^{+0.0799}_{-0.0821}$	1.693
All systematics, except calibration	$0.2756^{+0.0164}_{-0.0133}$	$-1.0481^{+0.0573}_{-0.0580}$	1.068
All systematics, except host term	$0.2738^{+0.0186}_{-0.0145}$	$-1.0644^{+0.0790}_{-0.0809}$	1.677
All systematics, fixing α, β[b]	$0.2656^{+0.0179}_{-0.0144}$	$-1.1168^{+0.0807}_{-0.0824}$	1.641
Contribution of different systematics:			
Calibration	$0.2750^{+0.0185}_{-0.0150}$	$-1.0581^{+0.0774}_{-0.0791}$	1.614
SN Ia model	$0.2767^{+0.0163}_{-0.0132}$	$-1.0403^{+0.0543}_{-0.0547}$	1.013
Peculiar velocities	$0.2761^{+0.0163}_{-0.0132}$	$-1.0452^{+0.0544}_{-0.0548}$	1.002
Malmquist bias	$0.2758^{+0.0163}_{-0.0132}$	$-1.0474^{+0.0548}_{-0.0553}$	1.014
Non SN Ia contamination	$0.2763^{+0.0163}_{-0.0132}$	$-1.0430^{+0.0543}_{-0.0546}$	1.000
Milky Way extinction	$0.2762^{+0.0164}_{-0.0133}$	$-1.0441^{+0.0553}_{-0.0557}$	1.023
SN redshift evolution	$0.2763^{+0.0163}_{-0.0132}$	$-1.0408^{+0.0544}_{-0.0547}$	1.017
Host galaxy term	$0.2762^{+0.0163}_{-0.0132}$	$-1.0453^{+0.0556}_{-0.0562}$	1.029
Calibration:			
Colors of BD 17° 4708	$0.2719^{+0.0170}_{-0.0137}$	$-1.0720^{+0.0639}_{-0.0639}$	1.239
SED of BD 17° 4708	$0.2771^{+0.0170}_{-0.0138}$	$-1.0390^{+0.0623}_{-0.0630}$	1.205
SNLS zeropoints	$0.2767^{+0.0168}_{-0.0136}$	$-1.0421^{+0.0603}_{-0.0609}$	1.166
Low-z zeropoints	$0.2753^{+0.0164}_{-0.0133}$	$-1.0527^{+0.0578}_{-0.0586}$	1.078
SDSS zeropoints	$0.2767^{+0.0164}_{-0.0133}$	$-1.0411^{+0.0544}_{-0.0548}$	1.015
SNLS filters	$0.2789^{+0.0170}_{-0.0138}$	$-1.0330^{+0.0585}_{-0.0586}$	1.136
Lowz filters	$0.2766^{+0.0163}_{-0.0132}$	$-1.0402^{+0.0547}_{-0.0550}$	1.010
SDSS filters	$0.2770^{+0.0164}_{-0.0133}$	$-1.0396^{+0.0544}_{-0.0548}$	1.007
HST zeropoints	$0.2769^{+0.0164}_{-0.0133}$	$-1.0412^{+0.0544}_{-0.0548}$	1.007
NICMOS nonlinearity	$0.2767^{+0.0164}_{-0.0133}$	$-1.0418^{+0.0545}_{-0.0548}$	1.009
SN Ia model (light curve fitter):			
SALT2 vs. SiFTO	$0.2767^{+0.0163}_{-0.0132}$	$-1.0404^{+0.0543}_{-0.0547}$	1.012
Color uncert. model	$0.2763^{+0.0163}_{-0.0132}$	$-1.0430^{+0.0543}_{-0.0546}$	1.001
SN Ia redshift evolution:			
α	$0.2763^{+0.0163}_{-0.0132}$	$-1.0430^{+0.0543}_{-0.0546}$	1.000

Table 3—Continued

Source	Ω_m	w	Relative area[a]
β	$0.2763^{+0.0163}_{-0.0132}$	$-1.0408^{+0.0544}_{-0.0547}$	1.017

[a]The area of the Ω_m–w 68.3% confidence contour relative to a fit considering statistical errors only. The contours are computed with the marginalization (grid) approach, include BAO and WMAP7 constraints, and assume a flat universe; see text for details.

[b]All our cosmological results have α and β free in the fits. This entry shows the effect of incorrectly holding them fixed.

Table 4. Cosmological results[a] obtained using the `CosmoMC` fitter with a constant dark energy equation of state

Parameter	WMAP7+SNLS3	WMAP7+DR7	WMAP7+$H0$[b]	WMAP7+DR7 +H_0	WMAP7+DR7 +SNLS3	WMAP7+DR7 +SNLS3+H_0
Flat, constant w:						
Ω_m	$0.262^{+0.023}_{-0.023}$	$0.329^{+0.034}_{-0.039}$	$0.246^{+0.020}_{-0.020}$	$0.267^{+0.017}_{-0.017}$	$0.284^{+0.019}_{-0.019}$	$0.269^{+0.015}_{-0.015}$
w	$-1.016^{+0.077}_{-0.079}$	$-0.826^{+0.166}_{-0.161}$	$-1.114^{+0.113}_{-0.113}$	$-1.110^{+0.122}_{-0.120}$	$-1.021^{+0.078}_{-0.079}$	$-1.061^{+0.069}_{-0.068}$
H_0	$71.58^{+2.41}_{-2.42}$	$64.42^{+4.25}_{-4.38}$	$74.11^{+2.58}_{-2.55}$	$72.21^{+2.46}_{-2.42}$	$69.77^{+2.07}_{-2.07}$	$71.57^{+1.65}_{-1.65}$
Non-flat, constant w:						
Ω_m	$0.259^{+0.050}_{-0.049}$	$0.312^{+0.051}_{-0.051}$	$\cdots$	$0.253^{+0.021}_{-0.021}$	$0.294^{+0.021}_{-0.021}$	$0.271^{+0.015}_{-0.015}$
Ω_k	$0.001^{+0.015}_{-0.015}$	$-0.006^{+0.013}_{-0.012}$	$\cdots$	$-0.012^{+0.008}_{-0.008}$	$-0.009^{+0.008}_{-0.008}$	$-0.002^{+0.006}_{-0.006}$
w	$-1.018^{+0.113}_{-0.110}$	$-1.027^{+0.379}_{-0.386}$	$\cdots$	$-1.445^{+0.298}_{-0.292}$	$-1.068^{+0.094}_{-0.095}$	$-1.069^{+0.091}_{-0.092}$
H_0	$72.65^{+6.59}_{-6.73}$	$66.36^{+5.73}_{-5.87}$	$\cdots$	$73.54^{+2.77}_{-2.79}$	$67.85^{+2.58}_{-2.57}$	$71.18^{+1.92}_{-1.87}$

[a]The values quoted are the expectation values of the marginalized distributions, not the best fits, with the 68.3% marginalized values quoted as the errors. All SN systematic uncertainties are included. Note that as the non-SN constraints used in `CosmoMC` differ slightly from those used in Table 2, the cosmological parameters are different. The closest comparison is SNLS3+WMAP7+DR7.

[b]We show only flat universe fits for the WMAP+H_0 combination; the fits were not constraining for non-flat cosmologies.

Table 5. The full set of cosmological parameters obtained with the `CosmoMC` fitter

Class	Parameter	Const. w flat	Const. w non-flat
Primary	$100\Omega_b h^2$	$2.258^{+0.054}_{-0.054}$	$2.265^{+0.056}_{-0.056}$
	Ω_c	$0.1149^{+0.0041}_{-0.0041}$	$0.1145^{+0.0047}_{-0.0047}$
	θ	$1.0398^{+0.0026}_{-0.0027}$	$1.0401^{+0.0026}_{-0.0026}$
	τ	$0.087^{+0.006}_{-0.007}$	$0.088^{+0.007}_{-0.007}$
	Ω_k	$\cdots$	$-0.002^{+0.006}_{-0.006}$
	w_0	$-1.061^{+0.069}_{-0.068}$	$-1.069^{+0.091}_{-0.092}$
	n_s	$0.969^{+0.013}_{-0.013}$	$0.970^{+0.014}_{-0.013}$
	$\log[10^{10}A_{05}]$	$3.095^{+0.033}_{-0.033}$	$3.094^{+0.033}_{-0.033}$
	α	$1.451^{+0.109}_{-0.109}$	$1.454^{+0.112}_{-0.111}$
	β	$3.265^{+0.111}_{-0.111}$	$3.259^{+0.111}_{-0.109}$
Derived	$\Omega_{\rm DE}$	$0.731^{+0.015}_{-0.015}$	$0.731^{+0.015}_{-0.015}$
	Age[a]	$13.71^{+0.11}_{-0.11}$ Gyr	$13.78^{+0.31}_{-0.31}$ Gyr
	Ω_m	$0.269^{+0.015}_{-0.015}$	$0.271^{+0.015}_{-0.015}$
	σ_8	$0.850^{+0.038}_{-0.038}$	$0.847^{+0.038}_{-0.038}$
	$z_{\rm re}$[b]	$10.55^{+1.20}_{-1.19}$	$10.55^{+1.20}_{-1.18}$
	H_0	$71.57^{+1.65}_{-1.65}$ km s^{-1} Mpc^{-1}	$71.18^{+1.92}_{-1.87}$ km s^{-1} Mpc^{-1}

[a]The current age of the universe

[b]The redshift at which the reionization fraction is a half

Table 6.   Cosmological results obtained with `CosmoMC` assuming a variable dark energy equation
of state and a flat universe

Parameter	WMAP7+DR7 +SNLS3	WMAP7+DR7 +SNLS3+H_0 (stat. only)	WMAP7+DR7 +SNLS3+H_0 (stat+sys)
Ω_m	$0.282^{+0.019}_{-0.019}$	$0.274^{+0.014}_{-0.014}$	$0.271^{+0.015}_{-0.015}$
w_0	$-0.949^{+0.198}_{-0.201}$	$-0.870^{+0.139}_{-0.139}$	$-0.905^{+0.196}_{-0.196}$
w_a	$-0.535^{+1.109}_{-1.111}$	$-0.938^{+0.821}_{-0.827}$	$-0.984^{+1.094}_{-1.097}$
H_0	$70.26^{+2.40}_{-2.43}$	$71.38^{+1.40}_{-1.38}$	$71.99^{+1.68}_{-1.69}$
FoM[a]	10.6	21.5	11.1

[a]The DETF (Albrecht et al. 2006) figure of merit (FoM), implemented here as $1/(\sigma_{w_p}\sigma_{w_a})$; see
§ 4.3.

Table 7.   Cosmological results fitting for a different w/Ω_m in each SNLS field

Fit	Ω_m	w	α	β	χ^2	r.m.s.
Basic fit	$0.272^{+0.017}_{-0.016}$	$-1.058^{+0.078}_{-0.082}$	$1.367^{+0.086}_{-0.084}$	$3.179^{+0.102}_{-0.099}$	418.1	0.153
4 field fit[a]	$0.265^{+0.105}_{-0.133}$, $0.311^{+0.095}_{-0.123}$, $0.241^{+0.111}_{-0.127}$, $0.268^{+0.100}_{-0.123}$	$-1.044^{+0.300}_{-0.300}$, $-1.235^{+0.312}_{-0.358}$, $-0.931^{+0.222}_{-0.245}$, $-1.058^{+0.258}_{-0.310}$	$1.356^{+0.086}_{-0.084}$	$3.183^{+0.103}_{-0.101}$	414.9	0.153

[a]Fitting for global nuisance parameters and a different Ω_m and w in each of the four SNLS fields. The
average values of the four Ω_m and w values are applied to non-SNLS SNe. See § 5.1 for details.

Table 8.   Fits for Ω_m and w using SN Ia sub-samples

Sample	N	α	β	M_B^1	M_B^2	σ_{diff}[a]	Ω_m	w	r.m.s.
Statistical:									
All[b]	368	1.354 ± 0.081	3.097 ± 0.094	-19.119 ± 0.020	-19.197 ± 0.016	5.1	0.281 ± 0.015	-1.013 ± 0.055	0.139
$s \leq 1.0$	174	1.736 ± 0.180	2.837 ± 0.141	-19.147 ± 0.031	-19.253 ± 0.029	4.1	0.280 ± 0.016	-1.020 ± 0.068	0.135
$s > 1.0$	194	1.998 ± 0.251	3.275 ± 0.136	-19.054 ± 0.034	-19.126 ± 0.029	3.3	0.284 ± 0.016	-0.994 ± 0.070	0.143
$C \leq 0.0$	178	1.462 ± 0.125	3.792 ± 0.370	-19.069 ± 0.036	-19.126 ± 0.028	2.0	0.284 ± 0.017	-0.990 ± 0.072	0.132
$C > 0.0$	190	1.267 ± 0.120	3.797 ± 0.197	-19.173 ± 0.031	-19.286 ± 0.026	4.4	0.281 ± 0.017	-1.012 ± 0.072	0.148
$\mathrm{M_{stellar}} \leq 10$	134	1.337 ± 0.199	3.575 ± 0.169	-19.142 ± 0.032	$\cdots$	$\cdots$	0.275 ± 0.017	-1.064 ± 0.090	0.141
$\mathrm{M_{stellar}} > 10$	234	1.319 ± 0.087	2.802 ± 0.114	$\cdots$	-19.185 ± 0.016	$\cdots$	0.283 ± 0.016	-0.990 ± 0.057	0.134
Statistical+Systematic:									
ALL	368	1.341 ± 0.082	3.084 ± 0.099	-19.128 ± 0.028	-19.193 ± 0.024	3.0	0.282 ± 0.018	-1.004 ± 0.084	0.138
$s \leq 1.0$	174	1.753 ± 0.185	2.895 ± 0.161	-19.142 ± 0.040	-19.260 ± 0.036	3.4	0.280 ± 0.018	-1.022 ± 0.093	0.137
$s > 1.0$	194	1.981 ± 0.254	3.246 ± 0.141	-19.063 ± 0.040	-19.133 ± 0.037	2.5	0.284 ± 0.019	-0.993 ± 0.098	0.143
$C \leq 0.0$	178	1.478 ± 0.135	3.981 ± 0.416	-19.077 ± 0.046	-19.118 ± 0.037	1.2	0.281 ± 0.020	-1.011 ± 0.109	0.135
$C > 0.0$	190	1.246 ± 0.123	3.826 ± 0.199	-19.191 ± 0.040	-19.297 ± 0.038	3.0	0.282 ± 0.020	-1.003 ± 0.107	0.149
$\mathrm{M_{stellar}} \leq 10$	134	1.320 ± 0.202	3.481 ± 0.178	-19.158 ± 0.043	$\cdots$	$\cdots$	0.272 ± 0.020	-1.085 ± 0.125	0.139
$\mathrm{M_{stellar}} > 10$	234	1.308 ± 0.089	2.854 ± 0.124	$\cdots$	-19.177 ± 0.024	$\cdots$	0.282 ± 0.018	-0.999 ± 0.084	0.134

[a]The significance of the difference between M_B^1 and M_B^2, including covariances.

[b]"ALL" means all SNe in the redshift restricted sample described in § 5.2.

Table 9.   Nuisance parameter variation for low and high M_{stellar} host galaxies. The σ columns give the significance of the difference in that nuisance parameter between the two host types.

Fit	α^1	α^2	σ_{diff}	β^1	β^2	σ_{diff}	M_B^1	M_B^2	σ_{diff}
Statistical:									
$1\alpha,1\beta,1M_B$	1.29 ± 0.08	$\cdots$	$\cdots$	3.15 ± 0.09	$\cdots$	$\cdots$	-19.188 ± 0.015	$\cdots$	$\cdots$
$1\alpha,1\beta,2M_B$	1.39 ± 0.08	$\cdots$	$\cdots$	3.14 ± 0.09	$\cdots$	$\cdots$	-19.130 ± 0.019	-19.203 ± 0.016	5.0
$1\alpha,2\beta,1M_B$	1.27 ± 0.08	$\cdots$	$\cdots$	3.70 ± 0.16	2.78 ± 0.11	4.7	-19.186 ± 0.015	$\cdots$	$\cdots$
$2\alpha,1\beta,1M_B$	1.10 ± 0.14	1.34 ± 0.09	1.5	3.16 ± 0.09	$\cdots$	$\cdots$	-19.191 ± 0.015	$\cdots$	$\cdots$
$1\alpha,2\beta,2M_B$	1.37 ± 0.08	$\cdots$	$\cdots$	3.64 ± 0.16	2.81 ± 0.11	4.3	-19.130 ± 0.019	-19.197 ± 0.015	4.7
$2\alpha,1\beta,2M_B$	1.43 ± 0.17	1.39 ± 0.09	0.2	3.14 ± 0.09	$\cdots$	$\cdots$	-19.128 ± 0.021	-19.203 ± 0.016	4.5
$2\alpha,2\beta,1M_B$	1.00 ± 0.15	1.34 ± 0.09	2.1	3.74 ± 0.17	2.79 ± 0.11	5.0	-19.190 ± 0.015	$\cdots$	$\cdots$
$2\alpha,2\beta,2M_B$	1.33 ± 0.17	1.38 ± 0.09	0.3	3.64 ± 0.16	2.81 ± 0.11	4.3	-19.133 ± 0.021	-19.198 ± 0.015	4.0
Statistical+Systematic[a] :									
$1\alpha,1\beta,1M_B$	1.28 ± 0.08	$\cdots$	$\cdots$	3.19 ± 0.10	$\cdots$	$\cdots$	-19.193 ± 0.022	$\cdots$	$\cdots$
$1\alpha,1\beta,2M_B$	1.39 ± 0.09	$\cdots$	$\cdots$	3.18 ± 0.10	$\cdots$	$\cdots$	-19.130 ± 0.025	-19.206 ± 0.022	4.6
$1\alpha,2\beta,1M_B$	1.27 ± 0.08	$\cdots$	$\cdots$	3.75 ± 0.17	2.80 ± 0.12	4.5	-19.179 ± 0.021	$\cdots$	$\cdots$
$2\alpha,1\beta,1M_B$	1.08 ± 0.14	1.33 ± 0.09	1.6	3.21 ± 0.10	$\cdots$	$\cdots$	-19.196 ± 0.022	$\cdots$	$\cdots$
$1\alpha,2\beta,2M_B$	1.36 ± 0.08	$\cdots$	$\cdots$	3.65 ± 0.17	2.85 ± 0.12	4.0	-19.127 ± 0.024	-19.198 ± 0.021	4.6
$2\alpha,1\beta,2M_B$	1.41 ± 0.17	1.38 ± 0.09	0.2	3.18 ± 0.10	$\cdots$	$\cdots$	-19.129 ± 0.026	-19.206 ± 0.022	4.6
$2\alpha,2\beta,1M_B$	0.98 ± 0.16	1.33 ± 0.09	2.1	3.78 ± 0.17	2.81 ± 0.12	4.7	-19.185 ± 0.021	$\cdots$	$\cdots$
$2\alpha,2\beta,2M_B$	1.31 ± 0.18	1.37 ± 0.09	0.3	3.65 ± 0.17	2.85 ± 0.12	4.1	-19.129 ± 0.025	-19.198 ± 0.021	4.2

[a]We exclude the host galaxy systematic term in these fits; see § 5.3 for details.

Table 10.   Cosmological fits including multiple nuisance parameters for low and high $M_{stellar}$ host galaxies

Fit	Ω_m	w	r.m.s.	χ^2/DOF
Statistical:				
$1\alpha,1\beta,1M_B$	0.269 ± 0.014	-1.094 ± 0.055	0.153	453.6/467
$1\alpha,1\beta,2M_B$	0.274 ± 0.014	-1.039 ± 0.054	0.152	429.6/466
$1\alpha,2\beta,1M_B$	0.271 ± 0.014	-1.072 ± 0.054	0.152	430.2/466
$2\alpha,1\beta,1M_B$	0.270 ± 0.014	-1.088 ± 0.055	0.152	450.8/466
$1\alpha,2\beta,2M_B$	0.274 ± 0.014	-1.034 ± 0.053	0.150	410.9/465
$2\alpha,1\beta,2M_B$	0.274 ± 0.014	-1.039 ± 0.054	0.153	429.7/465
$2\alpha,2\beta,1M_B$	0.272 ± 0.014	-1.064 ± 0.054	0.151	425.7/465
$2\alpha,2\beta,2M_B$	0.274 ± 0.014	-1.034 ± 0.053	0.150	410.7/464
Statistical+Systematic[a] :				
$1\alpha,1\beta,1M_B$	0.266 ± 0.016	-1.116 ± 0.081	0.154	448.4/467
$1\alpha,1\beta,2M_B$	0.273 ± 0.016	-1.055 ± 0.079	0.153	423.1/466
$1\alpha,2\beta,1M_B$	0.276 ± 0.016	-1.037 ± 0.076	0.153	425.3/466
$2\alpha,1\beta,1M_B$	0.267 ± 0.016	-1.111 ± 0.081	0.153	445.9/466
$1\alpha,2\beta,2M_B$	0.274 ± 0.016	-1.040 ± 0.075	0.151	405.4/465
$2\alpha,1\beta,2M_B$	0.272 ± 0.016	-1.054 ± 0.079	0.153	423.1/465
$2\alpha,2\beta,1M_B$	0.275 ± 0.016	-1.041 ± 0.076	0.152	421.1/465
$2\alpha,2\beta,2M_B$	0.274 ± 0.016	-1.040 ± 0.075	0.150	405.3/464

[a]We exclude the host galaxy systematic term in these fits; see § 5.3 for details.